NBSIR 77-1235

Some Aspects of Using A Scanning Electron Microsope for Total Dose Testing

K. F. Galloway and P. Roitman

Electronic Technology Division
Institute for Applied Technology
National Bureau of Standards
Washington, D.C. 20234

September 1977

Final

Prepared for

Defense Nuclear Agency
Washington, D.C. 20305

NBSIR 77-1235

SOME ASPECTS OF USING A SCANNING ELECTRON MICROSCOPE FOR TOTAL DOSE TESTING

K. F. Galloway and P. Roitman

Electronic Technology Division
Institute for Applied Technology
National Bureau of Standards
Washington, D.C. 20234

September 1977

Final

Prepared for
Defense Nuclear Agency
Washington, D.C. 20305

U.S. DEPARTMENT OF COMMERCE, Juanita M. Kreps, *Secretary*

Dr. Sidney Harman, *Under Secretary*

Jordan J. Baruch, *Assistant Secretary for Science and Technology*

NATIONAL BUREAU OF STANDARDS, Ernest Ambler, *Acting Director*

TABLE OF CONTENTS

LIST OF FIGURES

List of Figures (continued)

Page

Some Aspects of Using a Scanning Electron Microscope for Total Dose Testing

K. F. Galloway and P. Roitman*
Electronic Technology Division
Institute for Applied Technology
National Bureau of Standards
Washington, D.C. 20234

Abstract

This report addresses a number of aspects involved in using a Scanning Electron Microscope (SEM) for radiation testing of semiconductor devices. Problems associated with using the low energy electron beam to simulate ^{60}Co exposure and a method for estimating the total absorbed dose in critical device oxides are discussed. The method is based on the experimentally determined expression for electron energy dissipation versus penetration depth in solid materials of Everhart and Hoff. An appendix giving the method of estimating the total absorbed dose in a form suitable for ASTM deliberations is included.

1. Introduction

Low energy electron beams such as those used in a scanning electron microscope (SEM) have been used in a number of experiments to explore the effects of ionizing radiation on semiconductor devices.[1-11] The SEM has been suggested as an instrument which can be used to selectively irradiate devices directly at the wafer level and which can simulate the effects of ^{60}Co gamma irradiation.[12-15] This report addresses a number of aspects involved in using an SEM for radiation testing of semiconductor devices. In particular, problems associated with using the low energy electron beam to simulate ^{60}Co exposure and a method for estimating the total absorbed dose† in critical device oxides are discussed.

If the SEM irradiation is intended to simulate a ^{60}Co radiation exposure, at least three factors must be considered. 1) For a low energy electron beam, the depth-dose distribution through the oxide may be quite different from the assumed constant depth-dose distribution for ^{60}Co exposure. 2) An SEM properly adjusted for imaging using secondary electrons will not deliver a uniform electron flux to the specimen.

---

*NBS-NRC Postdoctoral Research Associate.

†In this report, the terms total dose and total absorbed dose are used to indicate the total energy divided by total mass. This is to be distinguished from the term absorbed dose which is generally defined as a point quantity.

3) The dose rate during a typical SEM exposure is considerably higher than typical ^{60}Co dose rates.

Due to the variation in depth-dose profiles of low energy electrons in device structures, careful attention must be given to the method used for determining the total absorbed dose. The energy deposited by the electron beam can be considered primarily as a mechanism for electron-hole pair production in the device materials. Since an electron of approximately 170 keV or greater is necessary for displacement damage in silicon, permanent bulk damage can be neglected for SEM electron irradiation. In metals and semiconductor materials, the pair formation will only result in a transient effect. However, the trapping of holes in the silicon dioxide and interface state build-up at the silicon-silicon dioxide interface can result from low energy electron exposure. These are also the effects usually associated with ^{60}Co exposure[16] where the total absorbed dose in the oxide is the radiation parameter which correlates with changes in device electrical parameters. For this reason, the method given in this report will be for estimating the total absorbed dose in the oxide. The method is based on the experimentally determined expression for electron energy dissipation versus penetration depth in materials with atomic numbers between 10 and 15 given by Everhart and Hoff.[17]

In the following sections, the calculational method for estimating the total absorbed dose and various graphs to facilitate the calculation are given, an example calculation is presented, and techniques and problems relevant to using an SEM for radiation testing are discussed. An appendix giving the method of estimating the total absorbed dose in semiconductor devices due to SEM electron radiation in a form suitable for ASTM deliberations is included.

2. Calculation of Total Absorbed Dose

Early work on the distribution of energy loss versus penetration depth for kilovolt electrons was done by Grün.[18] Grün experimentally determined the electron energy absorption as a function of penetration depth in air and demonstrated two important points. First, he obtained a relationship between the projected range of electrons, R_G, and the electron beam energy, E_B:

$$R_G = 4.57\ E_B^{1.75}\ , \qquad (1)$$

where R_G is expressed in micrograms per square centimeter[§] and E_B is expressed in kilo-electron volts. This expression is valid for 5 keV $\leq$ $E_B \leq$ 25 keV. Second, he showed that the shape of the depth-dose relation

[§]The unit of length used here is mass thickness - the product of material density and thickness. For example, a layered structure of 800 nm of aluminum and 200 nm of silicon dioxide would have a thickness of 260 $\mu g/cm^2$.

is practically invariant if the penetration distance is expressed as a function of R_G and the energy is expressed as a fraction of E_B.

Everhart and Hoff[17] extended these general conclusions to solids and obtained a generalized depth-dose curve for solid materials. They determined experimentally a depth-dose function by taking the steady-state electron-beam-induced current through the insulating layer of a metal-oxide-semiconductor structure as a measure of the energy dissipation in that layer. For structures of aluminum, silicon dioxide, and silicon, Everhart and Hoff found the projected range expression,

$$R_G = 3.98\ E_B^{1.75}\ , \tag{2}$$

to be accurate for 5 keV $\leq E_B \leq$ 25 keV. Figure 1 is a plot of projected range versus electron beam energy. They also found that for elements with an atomic number in the range 10 to 15 the energy dissipation per unit mass thickness is given by

$$\frac{dE}{dx} = \frac{(1-f_B)E_B\lambda(y)}{R_G}\ , \tag{3}$$

where f_B is the fraction of incident energy backscattered, typically taken as 0.1 (see Appendix A), $y = x/R_G$ where x is the penetration depth in micrograms per square centimeter, and

$$\lambda(y) = 0.60 + 6.21y - 12.40y^2 + 5.69y^3\ . \tag{4}$$

Equation 3 is plotted in figure 2 for several beam energies.

The work of Everhart and Hoff provides the basis for calculating the total absorbed dose in the oxide layers of semiconductor devices exposed in a scanning electron microscope.

If uniform electron flux over the rastered area (A_S in square centimeters) is assumed, the number of incident electrons per unit area (electrons per square centimeter) is

$$N = \frac{I_B t}{qA_s}\ , \tag{5}$$

where I_B is the electron beam current in amperes, t is the exposure time in seconds, and q is the charge per electron (1.6×10^{-19} coulombs per electron). Multiplying N by the area of the oxide layer of interest (A_O in square centimeters) gives the number of electrons incident on the oxide.

The energy deposited in the oxide per electron can be calculated from eq (3) by integrating from x_1, the distance from the device surface

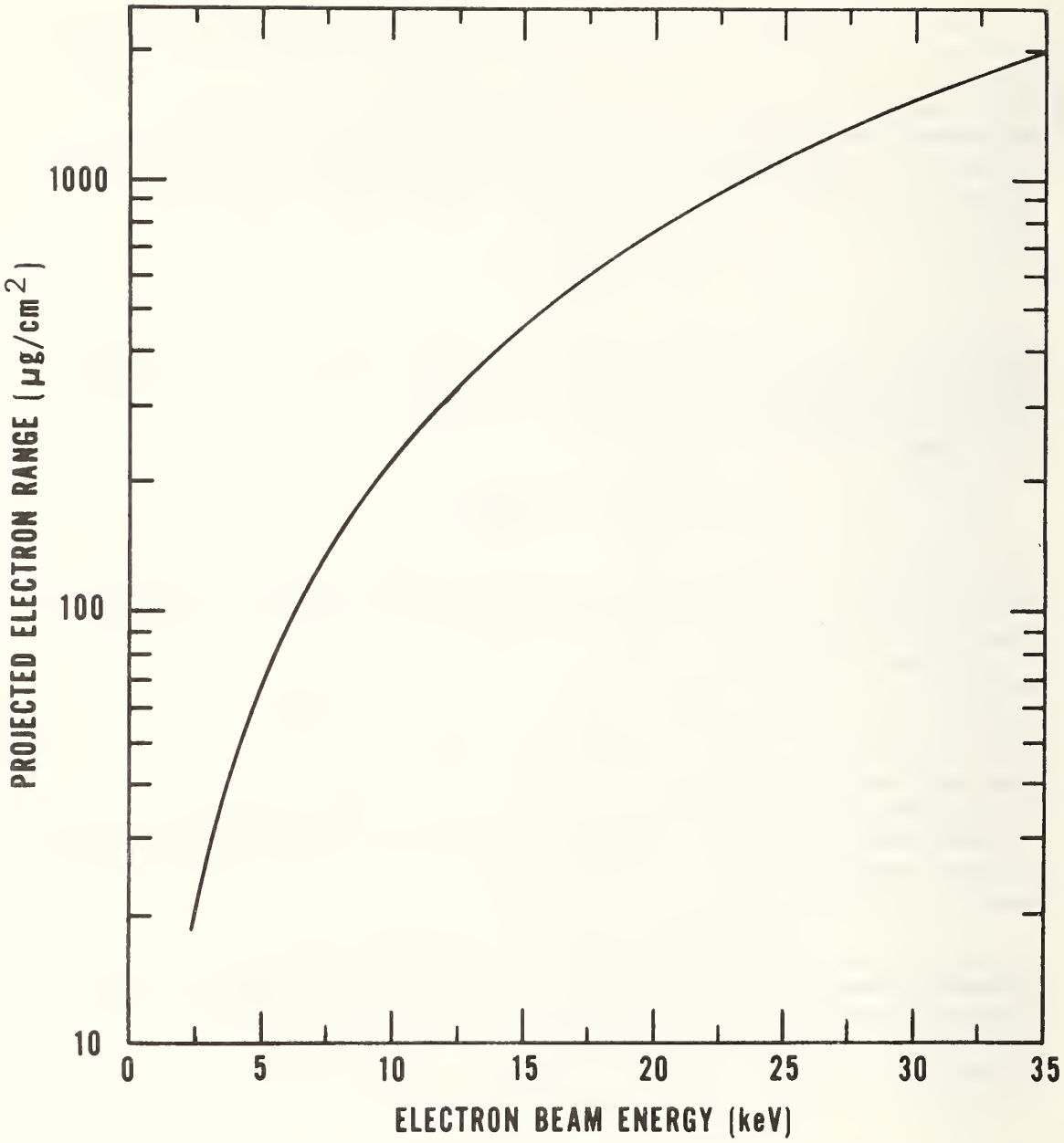

Figure 1. Projected electron range versus electron beam energy from the expression of Everhart and Hoff.

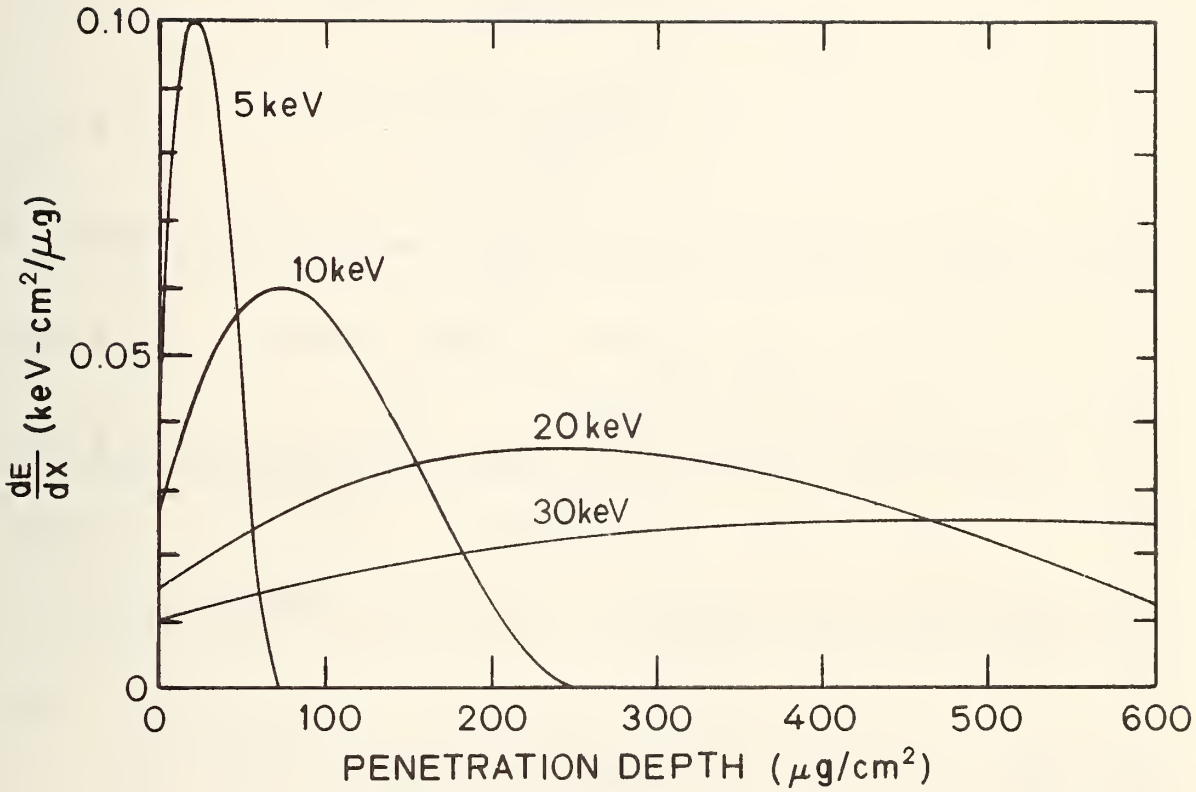

Figure 2. Energy deposition versus penetration depth for electron beams for four different energies based on the work of Everhart and Hoff. Ten percent of the beam energy is assumed to be back-scattered.

to the top of the oxide, to x_2, the distance to the bottom of the oxide. Normal incidence for the electron beam is assumed.

$$\begin{aligned} E_D &= \int_{x_1}^{x_2} \frac{dE}{dx}\, dx \\ &= (1-f_B)E_B \int_{y_1}^{y_2} \lambda(y)dy \\ &= (1-f_B)E_B\, [Y(y_2) - Y(y_1)] \\ &= (1-f_B)E_B\, f_D\ , \end{aligned} \tag{6}$$

where f_D is the fraction of incident electron energy deposited between y_1 and y_2 and

$$Y(y) = 0.6y + 3.105y^2 - 4.133y^3 + 1.425y^4\ . \tag{7}$$

Figure 3 is a plot of the function Y.

The total energy deposited in the oxide in kilo-electron volts is then

$$E_T = N \cdot A_o \cdot E_D\ . \tag{8}$$

The radiation dose in the oxide can be calculated by dividing E_T by the mass of the oxide layer in grams

$$M = A_o\ (x_2 - x_1)\ . \tag{9}$$

The result, in kilo-electron volts per microgram, is

$$\text{Dose} = N \cdot E_D \cdot (x_2 - x_1)^{-1}\ . \tag{10}$$

The commonly used unit of radiation dose, the rad, is defined as the amount of radiation which deposits 100 ergs of energy per gram of irradiated material; the total absorbed dose in the oxide layer in rad(SiO_2) is

$$\text{Dose [rad}(SiO_2)] = 1.602 \times 10^{-5}\ N \cdot E_D \cdot (x_2 - x_1)^{-1}\ . \tag{11}$$

The parameters used in determining N and E_D can be substituted explicitly in eq (11) and the total absorbed dose in the oxide layer can be expressed as

$$\text{Dose [rad}(SiO_2)] = \frac{10^{14}\ I_B E_B t(1-f_B)f_D}{A_s\ (x_2 - x_1)}\ . \tag{12}$$

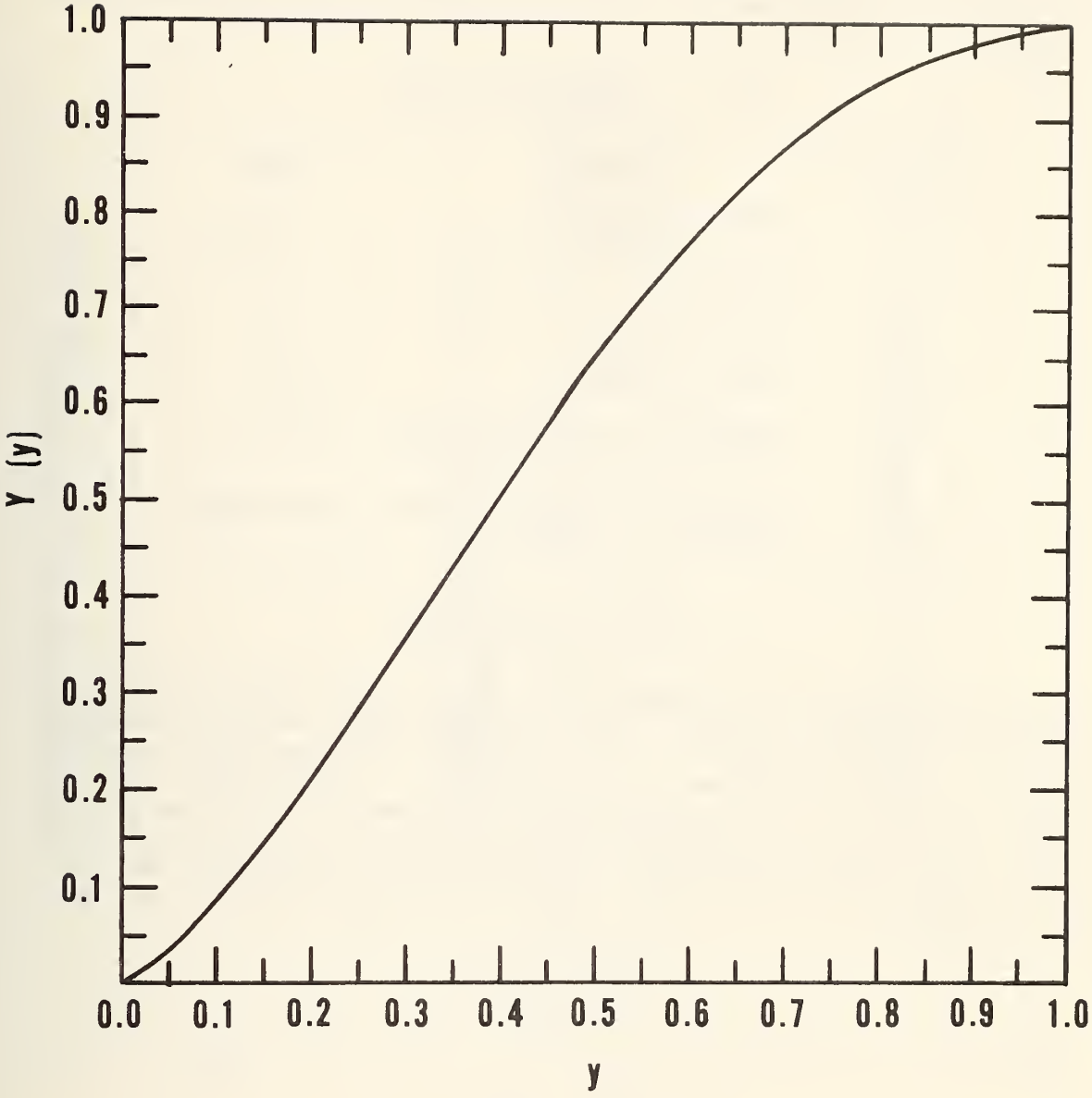

Figure 3. The function $Y(y) = 0.6\ y + 3.105\ y^2 - 4.133\ y^3 + 1.425\ y^4$ plotted as a function of y.

The quantities appearing in eq (12) and their units are given in table I.

Table I. SYMBOLS AND UNITS

Symbol	Parameter	Units
I_B	beam current	A
E_B	energy of beam electrons	keV
t	scan time	s
A_s	area of scan	cm^2
x_2-x_1	oxide thickness	$\mu g/cm^2$
f_B	fraction of incident energy backscattered from device	unitless
f_D	fraction of incident energy deposited in oxide	unitless

3. Example Calculation

Consider a critical oxide layer of 100 nm, for example the gate oxide of an MOS device, beneath 1 μm of aluminum which is in turn beneath a silicon oxide overcoat 1 μm thick. Figure 4 is a nomograph which can be used to convert aluminum, silicon dioxide, or aluminum plus silicon dioxide thickness in micrometers to mass thickness in micrograms per square centimeter. On a depth scale measured from the top of the overcoat, the critical oxide extends from 500 $\mu g/cm^2$ to 523 $\mu g/cm^2$ (x_1 and x_2, respectively). For a 20-keV electron beam, R_G is 752.8 $\mu g/cm^2$ (see fig. 1). Thus

$$y_1 = \frac{x_1}{R_G} = 0.664$$

$$y_2 = \frac{x_2}{R_G} = 0.695 \qquad (13)$$

and from eq (7)

$$Y(y_1) = 0.834$$

$$Y(y_2) = 0.861 \ . \qquad (14)$$

Thus, the energy deposited in the oxide expressed in kilo-electron volts per electron is

$$E_D = (1.0-0.1)\ 20\ [0.861-0.834]$$

$$= 0.486 \ . \qquad (15)$$

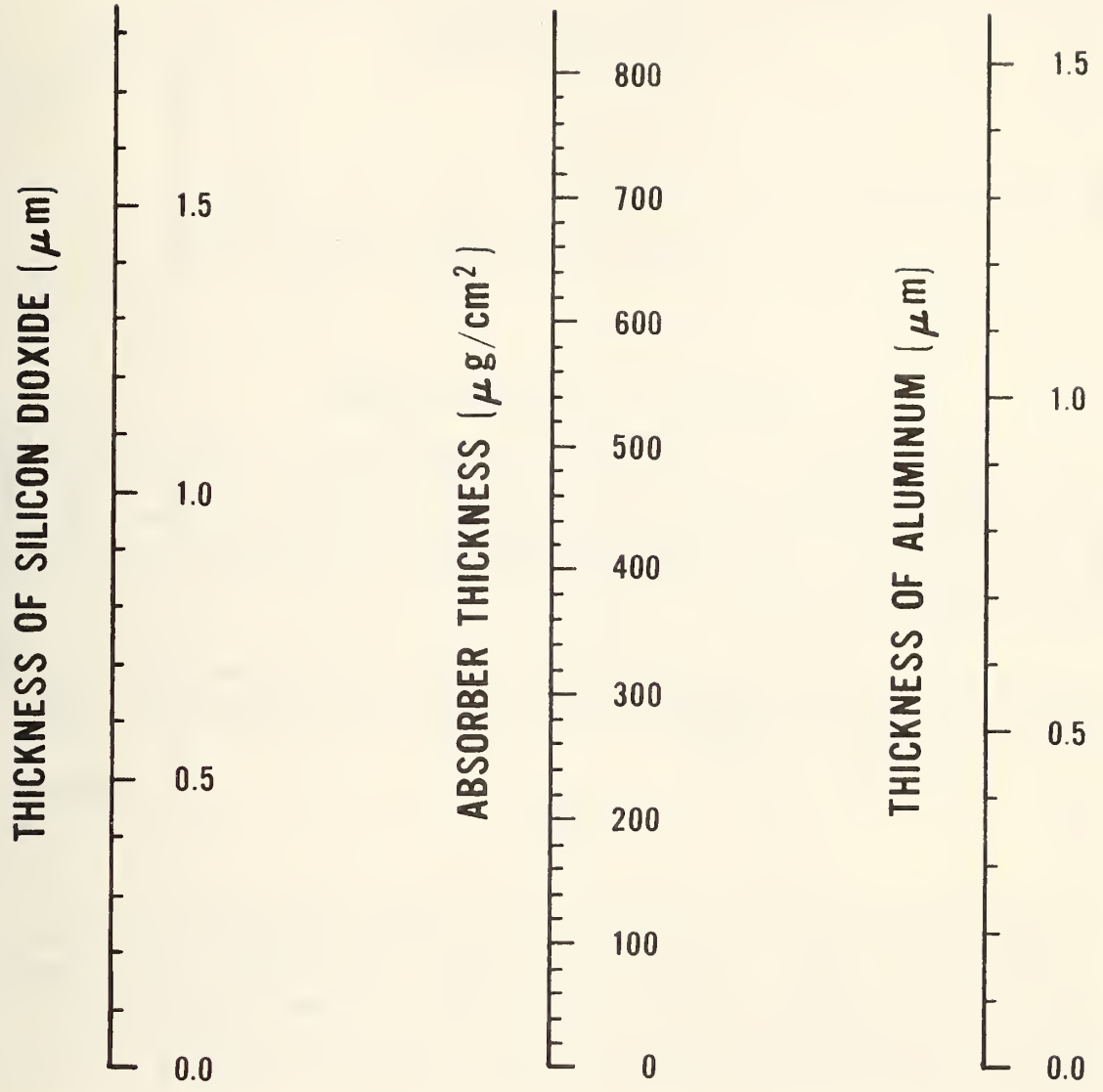

Figure 4. Nomograph for converting aluminum, silicon dioxide, or aluminum plus silicon dioxide thicknesses in micrometers to mass thickness in $\mu g/cm^2$. To use, draw a line from the silicon dioxide thickness in micrometers to the aluminum thickness in micrometers and read the absorber thickness in $\mu g/cm^2$.

For an electron beam of 100 pA scanning an area of 0.02 cm^2 for 100 s, the number of incident electrons per square centimeter is

$$N = \frac{(100 \times 10^{-12})\ (100)}{(1.6 \times 10^{-19})\ (.02)} = 3.125 \times 10^{12} \ . \tag{16}$$

The total absorbed dose in the oxide for this case is then

$$\text{Dose } [\text{rad}(SiO_2)] = \frac{(1.602 \times 10^{-5})\ (3.125 \times 10^{12})\ (0.486)}{23} = 1.06 \times 10^{6} \ . \tag{17}$$

4. Consideration of SEM Parameters

If the procedure for estimating the total absorbed dose outlined in the preceding sections is to yield reasonable results, the SEM should be adjusted so that the assumptions made in the calculation are met and the SEM parameters used in the calculation should be accurately determined. The requirement of a uniform electron flux incident on the specimen needs special attention.

The area of the specimen exposed to the electron beam or the area scanned, A_S, is usually related to the area of the recording CRT, A_{CRT}, and the SEM magnification by

$$A_s = \frac{A_{CRT}}{Mag} \ . \tag{18}$$

For this reason, the magnification needs to be accurately determined. The magnification is a function of many different variables and is usually determined using a calibration artifact. The electron beam current, I_B, is usually measured using a Faraday cup. The beam energy, E_B, is probably best determined from the x-rays emitted from a known target. Techniques for determining these and other critical parameters are discussed in a paper by Joy.[19]

In order that the assumption of uniform electron exposure be met, a number of factors must be carefully considered. The goal, of course, is a uniform dose deposited in the oxide layer. An SEM electron beam properly adjusted for secondary imaging is approximately circular in projection on the specimen with about 80 percent of the electrons in a circle 10 to 25 nm in diameter. As these electrons penetrate to the oxide layer of interest a radially varying dose distribution in the oxide results, primarily from multiple scattering of the electrons. Figure 5, taken from the work of Chadsey,[20] illustrates the radial dose distribution in the oxide for a point beam of 20-keV electrons incident on a 150-nm silicon dioxide layer on silicon beneath a 500-nm aluminum layer. Extrapolating from the data in this figure, it is obvious that when us-

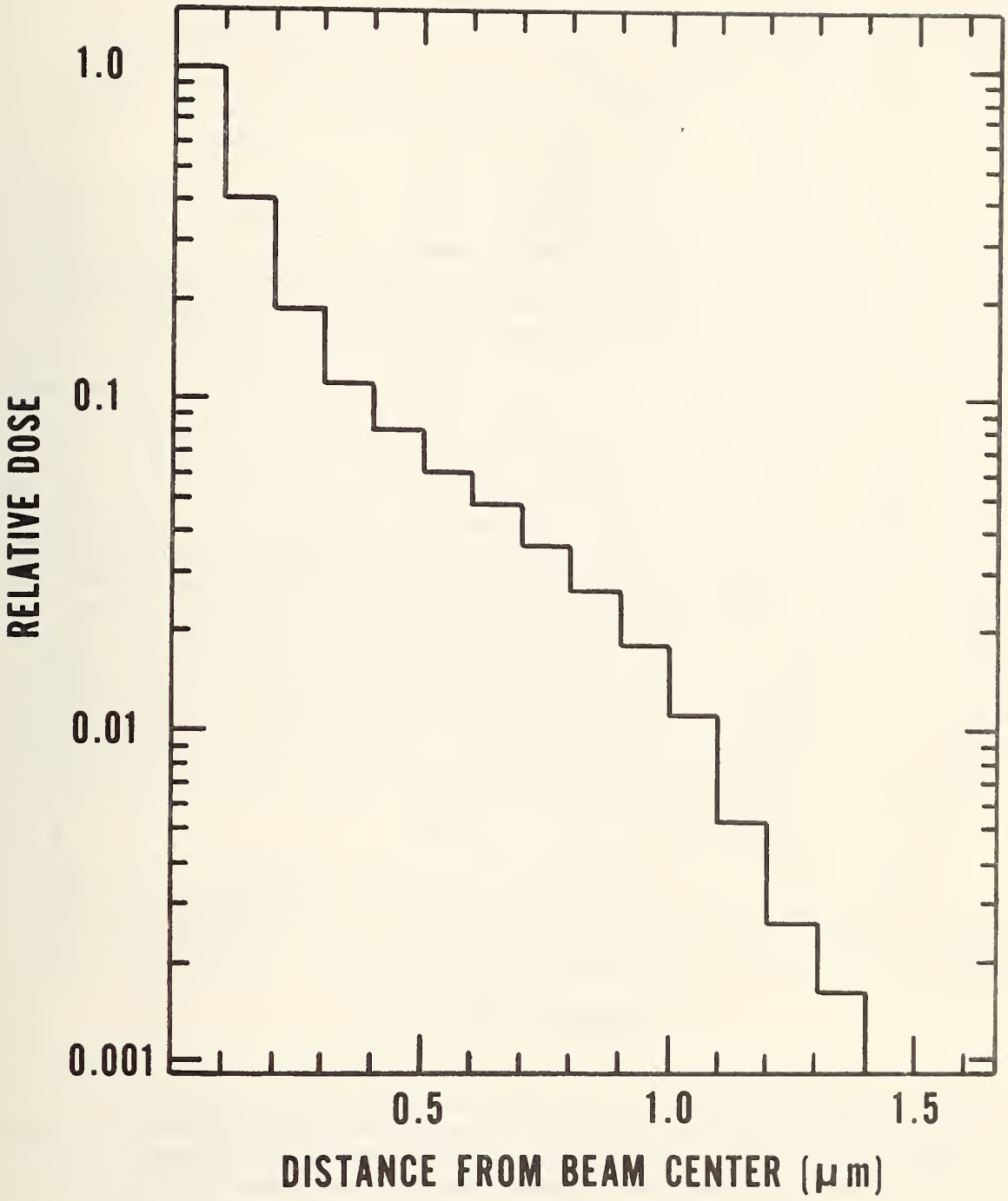

Figure 5. Relative radial dose distribution in the oxide layer for a point beam of 20-keV electrons incident on a 150-nm oxide layer beneath a 500-nm aluminum layer.

ing a well focused beam the scan lines must be on the order of 0.5 μm or less apart to achieve a uniform dose when irradiating typical chips. This is impractical since a typical chip to be exposed is on the order of 2500 μm on a side and the number of scan lines per frame is usually between 500 and 2000. Therefore, an SEM operated in its normal imaging mode will not deliver a uniform dose to typical device oxides.

This problem can be solved by defocusing the electron beam in order to obtain a uniform electron exposure. This is accomplished by decreasing the objective lens current. Beam diameters as large as 50 to 100 μm are easily attainable. Figure 6 illustrates beam "profiles" obtained by defocusing. The beam "profiles" shown in figure 6 were measured using an MOS induced current technique schematically shown in figure 7. An MOS capacitor with a gate 5 μm wide and several hundred micrometers long was oriented perpendicular to the scan direction and biased to accumulation. The current induced by the beam in the oxide was amplified and recorded on an x-y plotter. Figure 6a shows the profile of the gate at focus (beam diameter much less than gate width) and can be used to estimate the beam widths of the other traces. Figures 6b and 6c show the profiles obtained as the beam is progressively defocused. The amplitude is arbitrary as the beam current changes with objective lens setting. The beam current used to calculate the dose must be measured with the beam defocused. The profiles obtained in this way are not true beam intensity profiles as the gate integrates the electron distribution in one dimension. However, the full width of the measured profile, from where the current rises from zero to where it returns to zero, is exactly the full width of the beam plus the width of the gate stripe. Figure 8 represents the uniformity of exposure across a chip for electron beams with assumed Gaussian distributions of 0.025, 5.0, and $\geq$10.0 μm FWHM. If, for example, a 50-μm diameter beam is scanned across a chip on lines 5 μm apart, the resulting dose will be uniform.

Another factor to be considered is the time of exposure. If the time per frame is t_F and the time of exposure is t, the assumption of uniform exposure of the specimen is most nearly met if t is a rational multiple of t_F or if t is very much greater than t_F.

5. SEM Radiation Testing

This final section is devoted to a discussion of a number of other important details which must be considered when using an SEM for the radiation testing of semiconductor devices. Practical problems associated with device positioning, device biasing, and possible damage to adjacent devices are briefly addressed. Also, the effects of differences in depth-dose distribution and in dose rate between the low energy electrons from SEM exposure and the gamma-rays from ^{60}Co radiation testing are pointed out.

Positioning the device to be exposed in the SEM chamber may present a problem. This is particularly true if it is desired to expose only one or a few devices on a wafer. Some systems have optical viewing systems which are useful in positioning. It is also possible to

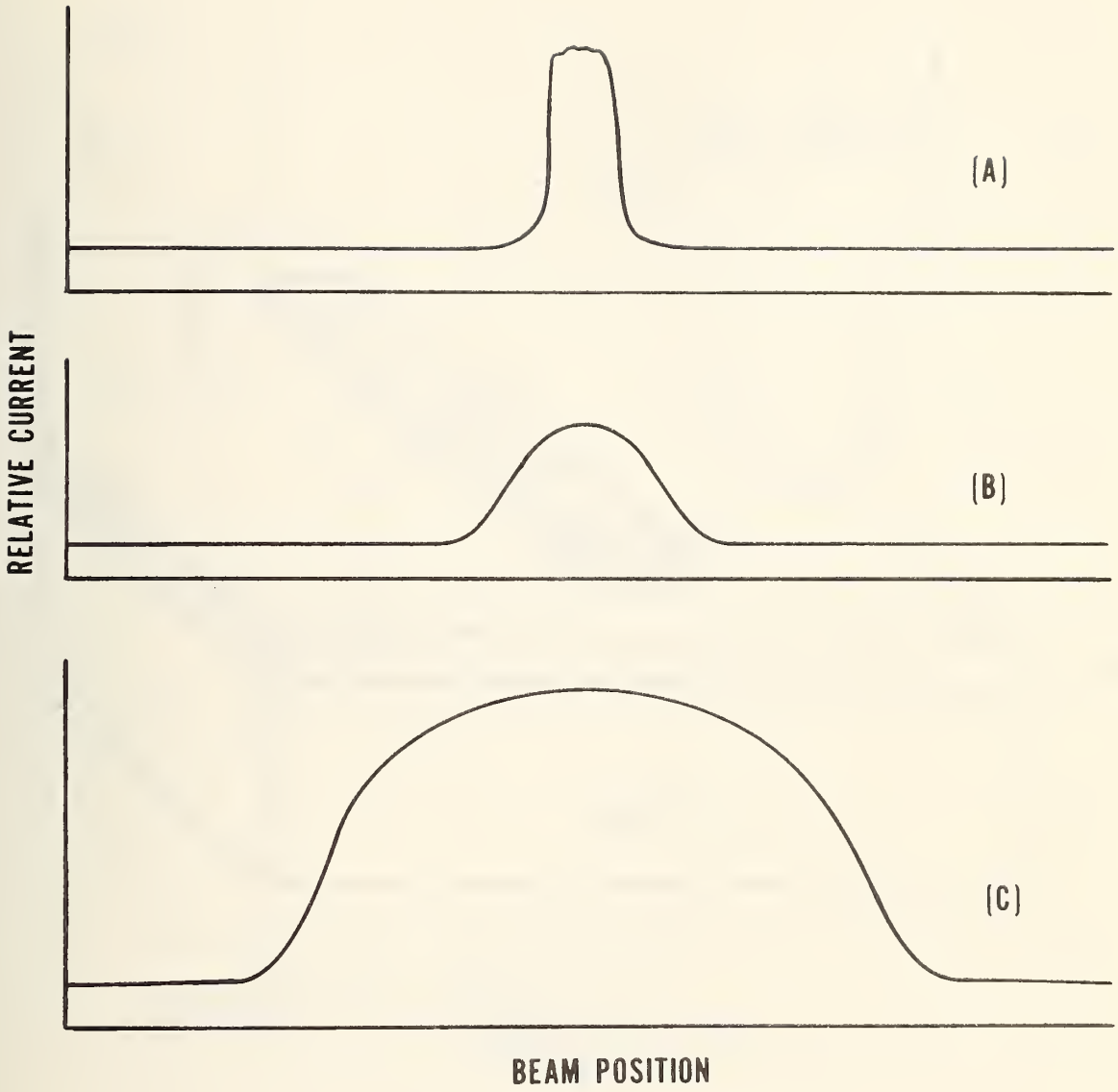

Figure 6. Beam "profiles" obtained by defocusing measured with a 5-μm aluminum stripe MOS capacitor. A. Focused beam; the width of the peak is approximately equal to the width of the 5-μm stripe. B. Beam width ∿4 μm. C. Beam width ∿18 μm.

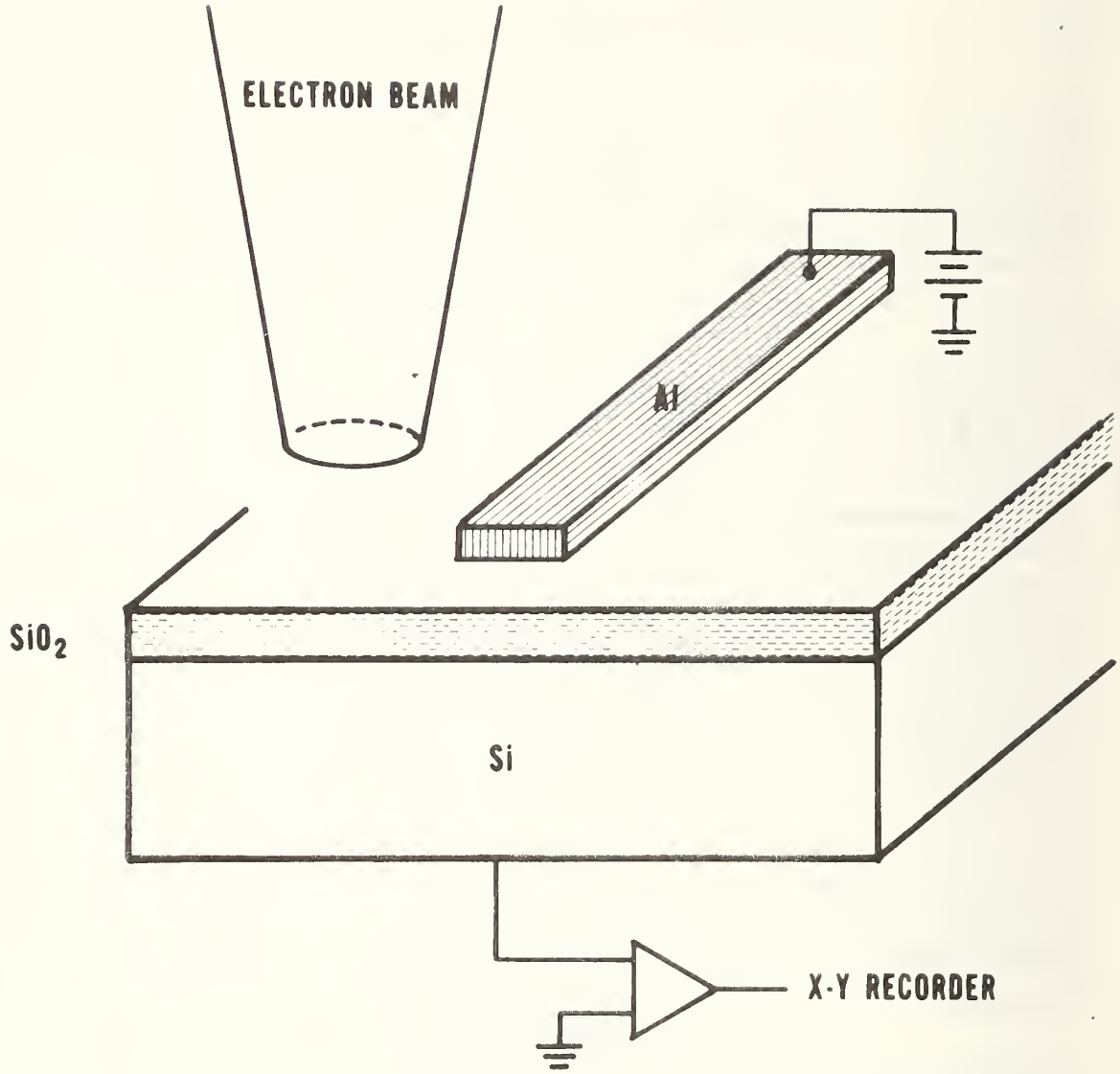

Figure 7. Schematic illustration of measurement arrangement for obtaining defocused "profiles" shown in figure 6.

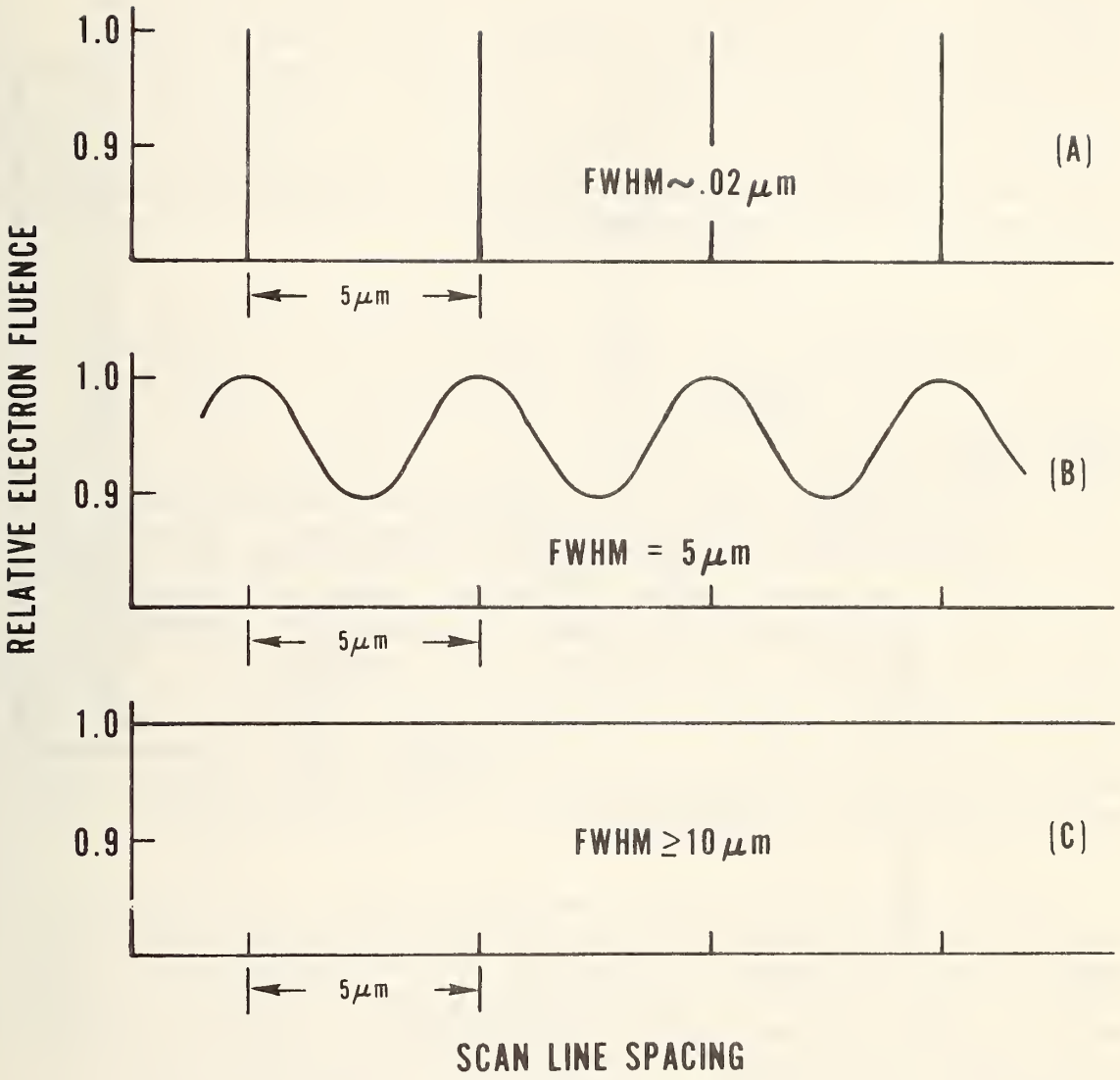

Figure 8. Relative electron fluence across the rastered area for three different beams with assumed Gaussian distributions. A. FWHM $\sim$ 0.2 μm. B. FWHM = 5 μm. C. FWHM $\geq$ 10 μm.

design and construct a fixture which will hold a wafer and provide shielding for those devices which are not to be exposed to the beam. In general, a very low energy electron beam ($E_B \leq 1$ keV) can be used to locate and align the device to be exposed. Electrons of this energy usually do not penetrate to critical oxide layers. However, a small but potentially significant number of continuum x-rays, generated by the electrons in the material covering the critical oxide layers, may penetrate to the oxide. If this technique is to be used, the exposure during set-up should be as short as possible. For a particular SEM system, it may be necessary to explore a number of techniques to discover the best method.

It is generally accepted that ionizing radiation effects are accentuated by applying bias to the device during the radiation exposure. Provisions for applying biases during SEM exposure to a single device mounted on a header are available in most instruments. However, SEM systems equipped with multiple probes for IC probing are not currently commercially available. A group interested in doing on-wafer failure analysis has designed a fixture which was mounted in an SEM chamber so that individual devices on a wafer could be biased during SEM irradiation.[21,22] The fixture, containing a probe card with the required number of probes, was rigidly mounted in the SEM chamber and aligned so that the region to be probed was centered on the electron optic axis. Figure 9 is a schematic illustration of this arrangement. The wafer is fixed in a specimen holder on the moveable stage of the SEM, and in operation, the chip to be investigated is adjusted relative to the probes and the wafer raised in the Z-direction until the probes mate with the pads. A system such as this would permit pre- and post-radiation electrical characterization and irradiation under bias of selected chips at the wafer level.

Another concern during wafer level irradiations is the possible damage to devices adjacent to the target device due to scattering of the electron beam in the target device or due to stray radiation in the SEM chamber. Using Monte Carlo techniques to examine the problem of scattering in the target device, Chadsey has shown that this effect is negligible in neighboring devices.[20] The magnitude of stray radiation in the SEM chamber is more difficult to predict. This background is due to electrons backscattered from the sample rescattering from the pole-piece and walls of the sample chamber. Measurements by Lipman *et al.*[12] indicated no effect on the gain of neighboring devices when the target device received a dose of approximately 1 Mrad(SiO_2). However, Ma *et al.*[10] in experiments on MOS capacitors observed an effect where the dose due to stray radiation can be estimated to be 10^{-3} to 10^{-5} times the dose in the target device.

In order to most closely simulate a ^{60}Co exposure with an SEM electron beam, the electron beam energy should be selected such that the energy dissipated per unit mass thickness (dE/dx) across the critical oxide is nearly constant. Exposure to ^{60}Co gamma-rays results in almost uniform energy deposition throughout a typical device. This is not the case for a low energy electron beam. Consider, for example, a critical

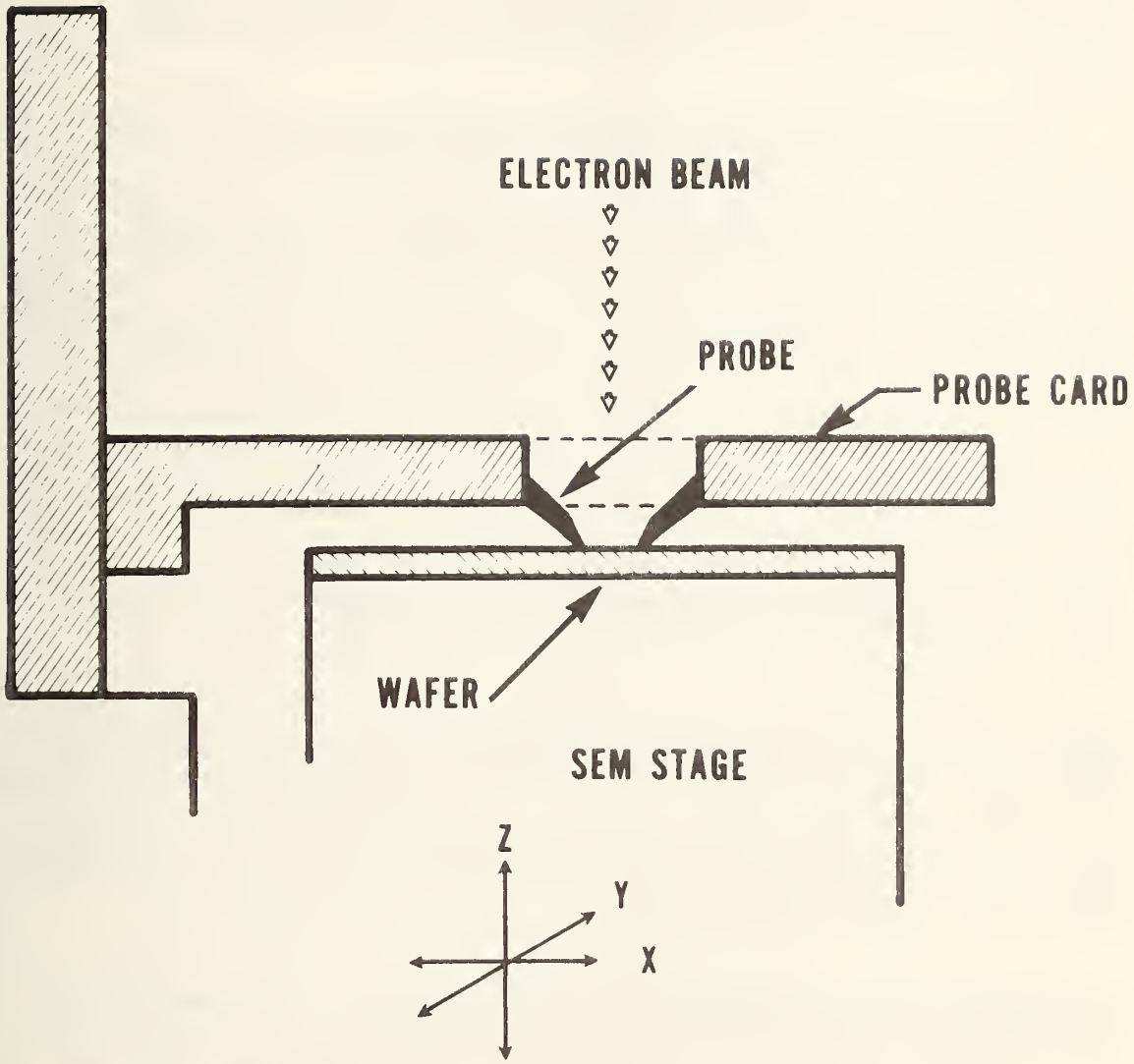

Figure 9. Schematic cross section through an SEM specimen chamber illustrating probe card arrangement for applying bias to an individual chip on a wafer.

oxide located between 200 and 250 μg/cm^2 in figure 2. A 5-keV beam will deposit no energy in this oxide layer. A 10-keV beam or a 20-keV beam could deposit the same amount of energy in this oxide layer if the individual times of exposure and beam currents were appropriately adjusted. However, the 20-keV beam deposits its energy more uniformly throughout the oxide. For this reason, a beam energy of 20 keV would be the better choice for simulating a ^{60}Co exposure for this particular device configuration.

Substantial differences in dose rate can exist between an SEM exposure and a ^{60}Co exposure delivering the same total dose to a device. Dose rate can be calculated from eq (12) using the raster scan time and the raster area or, equivalently, using the area of the beam spot and the time the beam spends on each spot if the electron exposure is uniform. A typical MOS gate oxide might be 100 nm thick under 1 μm of aluminum covered by 1 μm of glass. For a beam energy of 30 keV, a beam current of 100 pA, a raster area of 0.1 cm^2 (a chip of approximately 125 mils by 125 mils), and raster scan time of 1 s, the dose rate is 2.7×10^3 rad(SiO_2)/s. The beam current in the SEM may be varied conveniently from 1 pA to 10 nA, thereby varying the dose rate in a range of approximately 10 to 10^6 rad(SiO_2)/s. The lower limit is set by the reliability of the current-measuring electronics, assuming an image is not required during irradiation. The upper limit is set by the apertures of the SEM optics; beam currents of 10 μA or greater are obtainable if these apertures are removed (resolution will be lost). For comparison, typical dose rates for ^{60}Co exposures are 20 to 200 rad(SiO_2)/s.

Some dose rate effects have been reported for very high dose rates.[23] At the lower limits of SEM beam current the dose rate is comparable with ^{60}Co sources so those effects are clearly not a problem. In general, a consideration of the physics of device response would indicate that rate effects should not be significant at 10^4 to 10^5 rad/s. Above this rate, space charge effects may be important. Thus, radiation testing in the SEM offers the potential advantage of depositing significant doses in only a few minutes.

SEM radiation testing has been shown to yield results similar to ^{60}Co exposure for both bipolar[12] and MOS devices.[13] This technique has a unique feature in that the radiation sensitivity of different regions of an integrated circuit can be separately investigated.[15] When planning a program which is to include SEM radiation testing, reasonable simulation of ^{60}Co total dose exposure can be obtained if the various facets of SEM low energy electron irradiation are accounted for.

Acknowledgment

W. J. Keery, R. L. Pease, E. A. Wolicki, S. Othmer, J. R. Srour, and K. O. Leedy have offered suggestions and comments useful in the preparation of this report.

References

1. Green, D., Sandor, J. E., O'Keeffe, T. W., and Matta, R. K., Reversible Changes in Transistor Characteristics Caused by Scanning Electron Microscope Examination, *Appl. Phys. Lett.* 6, 3-4 (1965).

2. Thornton, P. R., Hughes, K. A., Kyaw, H., Millward, C., and Sulway, D. V., Failure Analysis of Microcircuitry by Scanning Electron Microscopy, *Microelectronics and Reliability* 6, 9 (1967).

3. Snow, E. H., Grove, A. S., and Fitzgerald, D. J., Effects of Ionizing Radiation on Oxidized Silicon Surfaces and Planar Devices, *Proc. IEEE* 55, 1168-1185 (1967).

4. Szedon, J. R., and Sandor, J. E., The Effect of Low-Energy Electron Irradiation of Metal-Oxide-Semiconductor Structures, *Appl. Phys. Lett.* 6, 181-182 (1965).

5. Speth, A. J., and Fang, F. F., Effects of Low-Energy Electron Irradiation on Si-Insulated Gate FETs, *Appl. Phys. Lett.* 7, 145-146 (1965).

6. Simons, M., Monteith, K. L., and Hauser, J. R., Some Observations on Charge Buildup and Release in Silicon Dioxide Irradiated with Low Energy Electrons, *IEEE Trans. Electron Devices* ED-15, 966-973 (1968).

7. MacDonald, N. C., and Everhart, T. E., Selective Electron-Beam Irradiation of Metal-Oxide-Semiconductor Structures, *J. Appl. Phys.* 39, 2433-2447 (1968).

8. MacDonald, N. C., Quantitative Scanning Electron Microscopy: Solid State Applications, *Scanning Electron Microscopy/1969*, pp. 431-437 (IIT Research Institute, Chicago, Illinois, 1969).

9. Thomas, A. G., Butler, S. R., Goldstein, J. I., and Parry, P. D., Electron Beam Irradiation Effects in Thick-Oxide MOS Capacitors, *IEEE Trans. Nucl. Sci.* NS-21, No. 4, 14-19 (1974).

10. Ma, T. P., Scoggan, G., and Leone, R., Comparison of Interface-State Generation by 25 keV Electron Beam Irradiation of p-type and n-type MOS Capacitors, *Appl. Phys. Lett.* 27, 61-63 (1975).

11. Ma, T. P., Oxide Thickness Dependence of Electron-Induced Surface States in MOS Structures, *Appl. Phys. Lett.* 27, 615-617 (1975).

12. Lipman, J. A., Bruncke, W. C., Crosthwait, D. L., Galloway, K. F., and Pease, R. L., Use of a Scanning Electron Microscope for Screening Bipolar Surface Effects, *IEEE Trans. Nucl. Sci.* NS-21, No. 6, 383-386 (1974).

13. Cohen, S., and Hughes, H., SEM Irradiation for Hardness Assurance Screening and Process Definition, *IEEE Trans. Nucl. Sci.* NS-21, No. 6, 387-389 (1974).

14. Lee, F., Improved Radiation Hardness of Bipolar Linear Circuits, *RCA Interim Report* (Contract No. N0014-74-C-0451), 1975.

15. Palkuti, L. J., Sivo, L. L., and Greegar, R. B., Process Investigations of Total-Dose, Hard, Type 108 OP Amps, *IEEE Trans. Nucl. Sci.* NS-23, 1756-1761 (1976).

16. Gwyn, C. W., Ionizing Radiation Effects in the Insulator Region of MOS Devices, Sandia Laboratories Report SLA-73-0013 (January 1973).

17. Everhart, T. E., and Hoff, P. H., Determination of Kilovolt Electron Energy Dissipation vs. Penetration Distance in Solid Materials, *J. Appl. Phys.* 42, 5837-5846 (1971).

18. Grün, A. E., Lumineszenz-Photometrische Messungen Der Energieabsorption in Strahlungsfeld von Elektronen Quellen Eindimensionaler Fall in Luft, *Z. Naturforsch.* 12A, 89-95 (1957).

19. Joy, D. C., SEM Parameters and Their Measurement, *Scanning Electron Microscopy/1974 (Part I)*, pp. 327-334 (IIT Research Institute, Chicago, Illinois, 1974).

20. Chadsey, W. L., Monte Carlo Calculations of Dose Distribution in SEM Irradiated Semiconductor Structures, NAD Crane Report TR/7024/C74/64 (October 1973).

21. Wolfgang, E., Otto, J., Kantz, D., and Linder, R., Stroboscopic Voltage Contrast of Dynamic 4096 BIT MOST RAMS: Failure Analysis and Function Testing, *Scanning Electron Microscopy/1976*, pp. 507-514 (IIT Research Institute, Chicago, Illinois, 1976).

22. Linder, R., Otto, J., and Wolfgang, E., On-Wafer Failure Analysis of LSI-MOS Memory Circuits by Scanning Electron Microscopy, *Siemens Forsch.-u. Entwickl.-Ber.* 6, 39-46 (1977).

23. Maier, R. J., and Tallon, R. W., Dose-Rate Effects in the Permanent Threshold Voltage Shifts of MOS Transistors, *IEEE Trans. Nucl. Sci.* NS-22, 2214-2218 (1975).

Appendix A

Analysis of the Fraction of Energy Backscattered

In order to utilize the energy deposited versus penetration results of Everhart and Hoff [A1] to calculate the energy deposited in aluminum, silicon dioxide, and silicon structures by a low energy electron beam, knowledge of the fraction of incident energy backscattered from the specimen (f_B) is necessary. This fraction is usually taken to be 0.1 from the work of Bishop [A2] at 30 keV. A study was undertaken to examine the validity of using this value at lower electron beam energies.

The fraction f_B depends on η, the fraction of incident electrons backscattered, and the fractional mean energy of the backscattered electrons:

$$f_B = \eta \, \bar{E}_{Bck}/E_B \ ,$$

where $\bar{E}_{Bck}$ is the mean energy of backscattered electrons and E_B is the beam energy. Both $\bar{E}_{Bck}/E_B$ and η depend on the incident energy, specimen composition, the incident beam angle, and the scattering angle at which they are measured. The data reviewed here are for normal incidence and are integrated over all possible scattering angles.

There have been several experimental determinations of η using a variety of experimental techniques [A3-A7]. In the energy range of interest here (usually $E_B \leq 30$ keV), the fraction of electrons backscattered from aluminum or silicon is almost independent of the beam energy, E_B, as shown in figure A1. Data on the fractional mean energy of backscattered electrons are scarce [A2,A8,A9]. Figure A2 illustrates the variation of $\bar{E}_{Bck}/E_B$ with beam energy for electrons backscattered from aluminum. The values given by Thomas [A8] were measured at 138 deg with respect to the beam direction; the average value over all backscattering angles would be greater. The values of f_B for an aluminum specimen can be calculated using these values of $\bar{E}_{Bck}/E_B$ and values of η from figure A1b interpolated when necessary to obtain values at the same energies. The results, with error bars estimated on the basis of scatter in the reported data, are shown in figure A3. It is apparent that taking the value of f_B to be 0.1 in the range 5 to 30 keV makes no more than a 2-percent contribution to the error in calculating the energy deposited. This contribution is small in comparison to the other possible sources of error. To a first approximation for silicon specimens, values of f_B can be taken to be the same as aluminum. The results are also expected to be applicable in general to devices consisting of silicon, silicon dioxide, and aluminum.

References

A1. Everhart, T. E., and Hoff, P. H., Determination of Kilovolt Electron Energy Dissipation vs. Penetration Depth in Solid Materials, *J. Appl. Phys.* 42, 5837-5846 (1971).

A2. Bishop, H. W., Electron Scattering in Thick Targets, *Brit. J. Appl. Phys.* 18, 703-715 (1967).

A3. Heinrich, K. F. J., Electron Probe Microanalysis by Specimen Current Measurement, *Proceedings of the Fourth International Congress of X-Ray Optics and Microanalysis*, R. Castaing, P. Deschamps, and J. Philibert, Eds., pp. 159-167 (Hermann, Paris, 1966).

A4. Colby, J. W., Wise, W. N., and Conley, D. K., Quantitative Microprobe Analysis by Means of Target Current Measurements, *Advan. X-Ray Anal.* 10, 447-461 (1967).

A5. Bishop, H. E., Electron Scattering and X-Ray Production, Ph.D. Dissertation, University of Cambridge (1966).

A6. Weinryb, E., and Philibert, J., Mesure du Coefficient de Rétrodiffusion des Electrons de 5 à 30 keV, *Compt. Rend.* 258, 4535-4538 (1964).

A7. Drescher, H., Reimer, L., and Seidel, H., Rückstreukoeffizient und Sekundärelektronen-Ausbeute von 10-100 keV-Elketronen und Beziehungen zur Raster-Elektronenmikroskopie, *Z. ang. Phys.* 29, 331-336 (1970).

A8. Thomas, R. N., Scattering of 5-20 keV Electrons in Metallic Films, Ph.D. Dissertation, University of Cambridge (1961).

A9. Darlington, E. H., Electron Backscattering at Low Energies, Ph.D. Dissertation, University of Cambridge (1970).

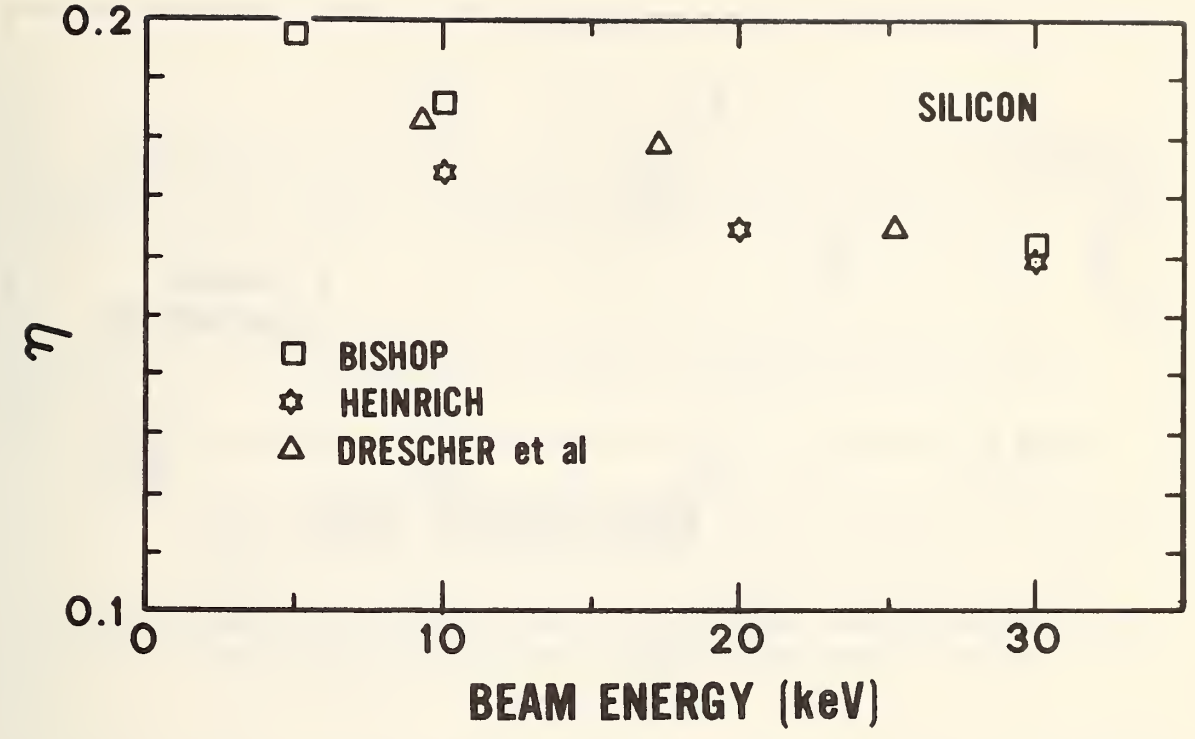

(a)

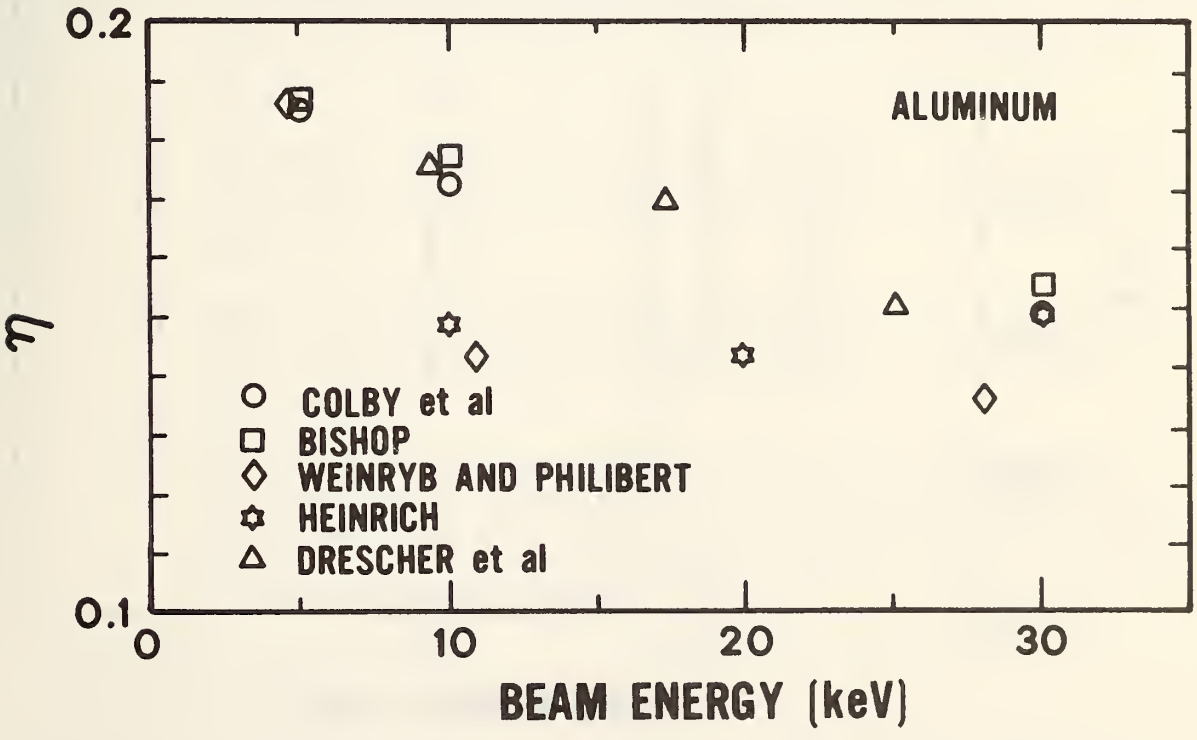

(b)

Al. Ratio of backscattered to incident electrons, η, as a function of beam energy. (a) Silicon specimen. (b) Aluminum specimen.

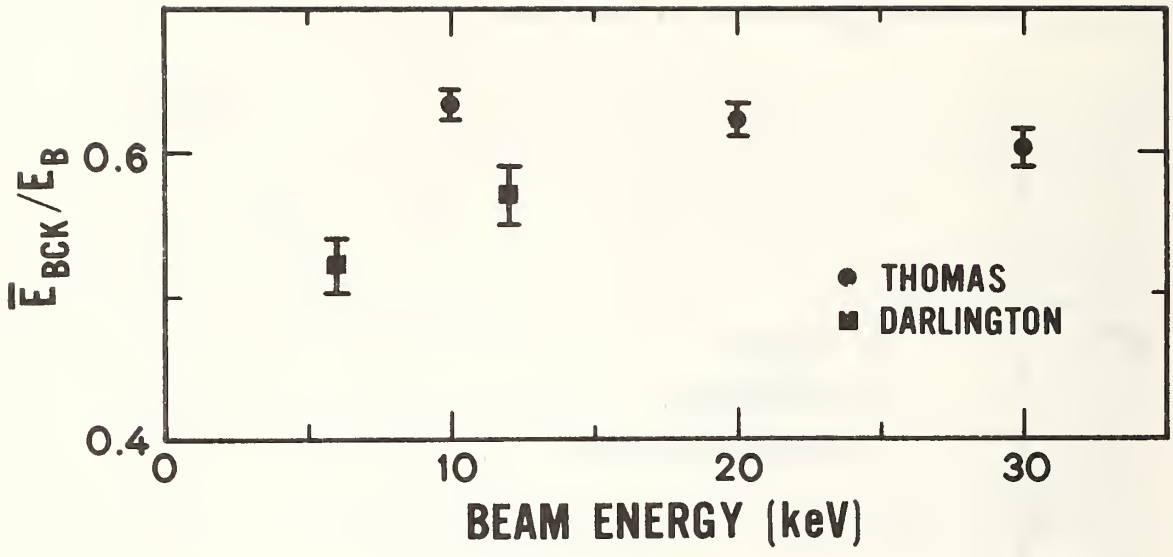

A2. Fractional mean energy backscattered, $\bar{E}_{Bck}/E_B$, from aluminum as a function of beam energy, E_B.

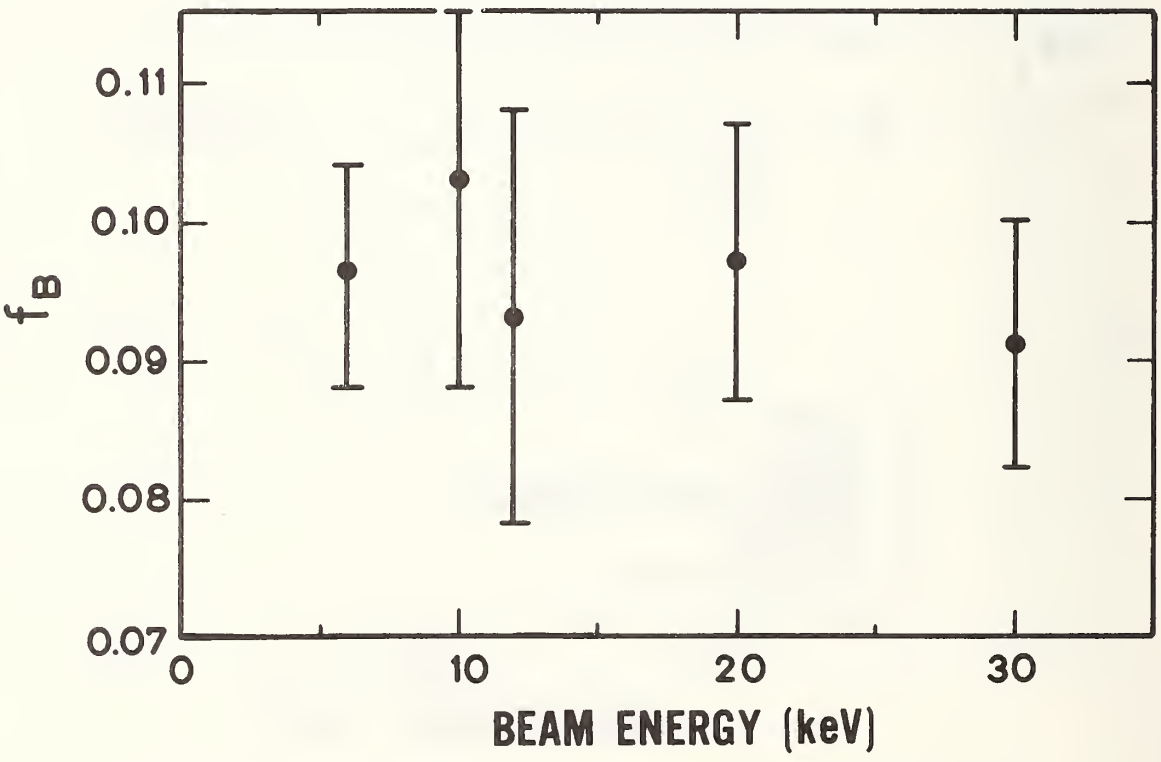

A3. Fraction of incident energy backscattered, f_B, from aluminum as a function of beam energy.

Appendix B

Draft of Recommended Practice

This appendix gives a method of estimating the total absorbed dose in semiconductor devices due to SEM electron irradiation in a form suitable as a first draft for presentation to Subcommittee F-1.11 on Quality and Hardness Assurance of ASTM Committee F-1 on Electronics.

Recommended Practice for Estimating the Total Absorbed Dose in Semiconductor Devices from SEM Electron Irradiation[1]

1. Scope

1.1 This recommended practice covers a method for calculating an estimation of the total absorbed dose in critical semiconductor device oxides resulting from exposure to the low energy electron beam available in a scanning electron microscope (SEM). The calculation is based on the experimental work on energy dissipation versus electron penetration depth of Everhart and Hoff (1).[2]

1.2 The calculation requires knowledge of the geometry and composition of the device structure and the parameters associated with the scanning electron microscope exposure: the electron beam energy, the electron beam current, the duration of the exposure, and the area scanned by the electron beam.

1.3 This method is limited to devices fabricated from materials with atomic numbers between 10 and 15. Thus, it is applicable to devices consisting of silicon, silicon oxides, silicon nitrides, and aluminum.

1.4 The experimental measurements of Everhart and Hoff were limited to electron energies between 5 and 25 keV. An extrapolation of these results to 40 keV is expected to incur only a small error.

1.5 This method assumes that the scanning electron microscope is adjusted so that the electron fluence incident on the device is uniform, that the electron beam is incident normally on the device, and that 10% of the incident energy is backscattered from the surface of the device (2).

---

[1]Reserved for ASTM jurisdictional footnote.

[2]The bold face numbers in parentheses refer to the list of references appended to this practice.

2. Significance

2.1 Knowledge of the effects of a total ionizing dose on the electrical characteristics of a semiconductor device is a requirement for many applications. Total absorbed dose testing is typically accomplished using ^{60}Co irradiation; however, it is often more convenient to simulate the exposure of a device to ^{60}Co gamma rays with an SEM than to use a ^{60}Co source.

2.2 The variation of dose with depth through the device for the SEM electron beam is dependent on the device structure and the beam energy; this variation may be quite different from the essentially constant depth-dose distribution for ^{60}Co exposure.

2.3 This practice takes account of the variations in depth-dose profiles of low energy electrons in device structures in the calculation of the total absorbed dose in critical device oxides.

3. Calculation

3.1 Calculate the number of incident electrons per unit area

$$N = \frac{I_B t}{q A_s}$$

where:

N = electron fluence, electrons/cm^2

I_B = electron beam current, A,

t = exposure time, s,

A_s = area scanned, cm^2, and

q = 1.6×10^{-19} C/electron.

3.2 Determine the projected range of the incident electrons

$$R_G = 3.98\ E_B^{1.75}$$

where:

R_G = electron projected range, $\mu g/cm^2$, and

E_B = electron beam energy, keV.

3.3 Using knowledge of the device structure, determine x_1, the distance from the device surface to the top of the oxide of interest, and x_2, the distance to the bottom of the oxide both in micrograms per square centimeter.

$$x_1 = \Sigma \rho_j d_j$$

$$x_2 = x_1 + \rho_o d_o$$

where:

ρ_j = density of layer j above oxide, $\mu g/cm^3$,
d_j = thickness of layer j above oxide, cm,
ρ_o = density of oxide layer, $\mu g/cm^3$, and
d_o = thickness of oxide layer, cm.

3.4 Calculate y_1 and y_2

$$y_1 = \frac{x_1}{R_G}, \quad y_2 = \frac{x_2}{R_G}$$

3.5 If $x_2 > R_G$, $y_2 = 1.0$. The electron beam is not penetrating the oxide layer. The results may be anomalous. Reconsider beam energy being used.

3.6 If $x_2 > R_G$, the dose in the oxide layer equals zero; stop the calculation.

3.7 If $x_1 \leq R_G$, continue with the calculation.

3.8 Calculate the fraction of incident electron energy deposited between y_1 and y_2

$$f_D = Y(y_2) - Y(y_1)$$

where:

f_D = fraction of incident energy deposited and

$$Y(y) = 0.6\ y + 3.105y^2 - 4.133y^3 + 1.425y^4$$

3.9 Calculate the energy deposited in the oxide layer per incident electron

$$E_D = 0.9\ E_B f_D$$

where:

E_D = energy deposited per electron, keV/electron.

3.10 Calculate the total absorbed dose in the oxide

$$D[\text{rad}(SiO_2)] = 1.602 \times 10^{-5}\ N \cdot E_D \cdot (x_2 - x_1)^{-1}$$

References

1. Everhart, T. E., and Hoff, P. E., Determination of Kilovolt Energy Dissipation vs. Penetration Distance in Solid Materials, *J. Appl. Phys.* 42, 5837-5846 (1971).

2. Galloway, K. F., and Roitman, P., Some Aspects of Using a Scanning Electron Microscope for Total Dose Testing, NBSIR 77-1235 (1977).

Defense Communication Engineer Center
1860 Wiehle Avenue
Reston, VA 22090
ATTN R410 James W. McLean

Director
Defense Communications Agency
Washington, D.C. 20305
ATTN Code 930 Monte T. Burgett, Jr.

Defense Documentation Center
Cameron Station
Alexandria, VA 22314
ATTN TC (12 copies)

Director
Defense Electronic Supply Center
Dayton, OH 45444
ATTN ECS Robert E. Cooper
ATTN ECS Joseph Dennis

Director
Defense Nuclear Agency
Washington, D.C. 20305
ATTN STTL Tech Library (3 copies)
ATTN STVL
ATTN DDST
ATTN RAEV
ATTN RAEV Maj. W. Adams (2 copies)

Dir of Defense Rsch & Engineering
Department of Defense
Washington, D.C. 20301
ATTN DDR&E(OS)

Commander
Field Command
Defense Nuclear Agency
Kirtland AFB, NM 87115
ATTN FCPR

Director
Interservice Nuclear Weapons School
Kirtland AFB, NM 87115
ATTN Document Control

Director
Joint Strat TGT Planning Staff JCS
Offutt AFB
Omaha, NB 68113
ATTN JLTW-2

Chief
Livermore Division Fld Command DNA
Lawrence Livermore Laboratory
P.O. Box 808
Livermore, CA 94550
ATTN FCPRL

Project Manager
Army Tactical Data Systems
U.S. Army Electronics Command
Fort Monmouth, NJ 07703
ATTN Dwaine B. Huewe

Commander
BMD System Command
P.O. Box 1500
Huntsville, AL 35807
ATTN BDMSC-TEN Noah J. Hurst

Commander
Frankford Arsenal
Bridge and Tacony Streets
Philadelphia, PA 19137
ATTN SARFA-FCD Marvin Elnick

Commander
Harry Diamond Laboratories
2800 Powder Mill Road
Adelphi, MD 20783
ATTN DRXDO-EM R. Bostak
ATTN DRXDO-RC Robert B. Oswald, Jr.
ATTN DRXDO-EM J. W. Beilfuss
ATTN DRXDO-EM Robert E. McCoskey
ATTN DRXDO-NP Francis N. Wimenitz
ATTN DRXDO-RBG Joseph Halpin
ATTN DRXDO-RB Joseph R. Miletta
ATTN DRXDO-TI Tech Lib

Commanding Officer
Night Vision Laboratory
U.S. Army Electronics Command
Fort Belvoir, VA 22060
ATTN Capt. Allan S. Parker

Commander
Picatinny Arsenal
Dover, NJ 07801
ATTN SMUPA-ND-D-E
ATTN SMUPA-ND-W

Commander
Redstone Scientific Information Ctr
U.S. Army Missile Command
Redstone Arsenal, AL 35809
ATTN Chief, Documents (3 copies)

Secretary of the Army
Washington, D.C. 20310
ATTN ODUSA or Daniel Willard

Commander
TRASANA
White Sands Missile Range, NM 88002
ATTN ATAA-EAC Francis N. Winans

Chief
U.S. Army Communications Sys Agency
Fort Monmouth, NJ 07703
ATTN SCCM-AD-SV Library

Commander
U.S. Army Electronics Command
Fort Monmouth, NJ 07703
ATTN DRSEL-GG-TD W. R. Werk
ATTN DRSEL-TL-IR Edwin T. Hunter
ATTN DRSEL-PL-ENV Hans A. Bomke

Commander-in-Chief
U.S. Army Europe and Seventh Army
APO New York 09403
ATTN ODCSE-E AEAGE-PI

Commander
U.S. Army Materiel Dev & Readiness Cmd
5001 Eisenhower Avenue
Alexandria, VA 22333
ATTN DRCDE-D Lawrence Flynn

Commander
U.S. Army Missile Command
Redstone Arsenal, AL 35809
ATTN DRCPM-PE-EA Wallace O. Wagner
ATTN DRCPM-LCEX Howard H. Henriksen
ATTN DRCPM-MDTI Capt. Joe A. Sims
ATTN DRSMI-RGD Victor W. Ruwe

Commander
U.S. Army Mobility Equip R&D Ctr
Fort Belvoir, VA 22060
ATTN STSFB-MW John W. Bond, Jr.
ATTN AMSEL-NV-SD J. H. Carter

Chief
U.S. Army Nuc and Chemical Surety Gp
Bldg. 2073, North Area
Ft. Belvoir, VA 22060
ATTN MOSG-ND Maj. Sidney W. Winslow

Commander
U.S. Army Nuclear Agency
Fort Bliss, TX 79916
ATTN ATCN-W LTC Leonard A. Sluga

Commander
U.S. Army Test and Evaluation Comd
Aberdeen Proving Ground, MD 21005
ATTN DRSTE-EL Richard I. Kolchin
ATTN DRSTE-NB Russell R. Galasso

Commander
White Sands Missile Range
White Sands Missile Range, NM 88002
ATTN STEWS-TE-NT Marvin P. Squires
ATTN Nuclear Effects Lab Ted F. Leura, Jr.

Commander
Naval Electronic Systems Command
Naval Electronic Systems Cmd Hqs
Washington, D.C. 20360
ATTN CODE 50451
ATTN ELEX 05323 Cleveland F. Watkins
ATTN CODE 504511 Charles R. Suman
ATTN PME 117-21
ATTN CODE 5032 Charles W. Neill

Director
Naval Research Laboratory
Washington, D.C. 20375
ATTN CODE 2627 Doris R. Folen
ATTN CODE 6601 E. Wolicki
ATTN CODE 5216 Harold L. Hughes
ATTN CODE 5210 John E. Davey
ATTN CODE 6620 Bruce Faraday
ATTN CODE 6627 Neal Wilsey

Commander
Naval Sea Systems Command
Navy Department
Washington, D.C. 20362
ATTN SEA-9931 Samuel A. Barham
ATTN SEA-9931 Riley B. Lane

Commander
Naval Surface Weapons Center
White Oak, Silver Spring, MD 20910
ATTN CODE WX21 Tech Lib
ATTN CODE WA50 John H. Malloy
ATTN CODE 244
ATTN CODE 431 Edwin B. Dean
ATTN CODE WA501 Navy Nuc Prgms Off
ATTN CODE WA52 Fred Warnock

Commander
Naval Weapons Center
China Lake, CA 93555
ATTN CODE 533 Tech Lib

Commanding Officer
Naval Weapons Support Center
Crane, IN 47522
ATTN CODE 3073 James Ramsey
ATTN CODE 3073 Joseph A. Munarin

Director
Strategic Systems Project Office
Navy Department
Washington, D.C. 20376
ATTN NSP-27331 Phil Spector
ATTN NSP-2342 Richard L. Coleman
ATTN NSP-230 David Gold
ATTN SP 2701 John W. Pitsenberger

Director
Office of Naval Research
800 N. Quincy Street
Arlington, VA 22217
ATTN 220 David Lewis

AF Aero-Propulsion Laboratory, AFSC
Wright-Patterson AFB, OH 45433
ATTN POE-2 Joseph F. Wise

AF Institute of Technology, AU
Wright-Patterson AFB, OH 45433
ATTN ENP Charles J. Bridgman

AF Materials Laboratory, AFSC
Wright-Patterson AFB, OH 45433
ATTN LTE

AF Weapons Laboratory, AFSC
Kirtland AFB, NM 87117
ATTN ELP TREE Section
ATTN ELA
ATTN SAS
ATTN ELP Capt. John G. Tucker
ATTN SAT
ATTN SAB
ATTN ELPT John Mullis
ATTN ELPT David Ferry

AFTAC
Patrick AFB, FL 32925
ATTN TFS Maj. Marion F. Schneider

Commander
ASD
Wright-Patterson AFB, OH 45433
ATTN ASD-YH-EX LTC Robert Leverette

Headquarters
Electronic Systems Division (AFSC)
Hanscom AFB, MA 01731
ATTN DCD/SATIN IV
ATTN YSEV
ATTN YWET

Commander
Foreign Technology Division, AFSC
Wright-Patterson AFB, OH 45433
ATTN ETET Capt. Richard C. Husemann

Commander
Rome Air Development Center, AFSC
Griffiss AFB, NY 13440
ATTN RBRAC I. L. Krulac
ATTN RBRP Jack S. Smith
ATTN RBRP Clyde Lane
ATTN RBRP Joseph Brauer

SAMSO/DY
Post Office Box 93960
Worldway Postal Center
Los Angeles, CA 90009
ATTN DYS Maj. Larry A. Darda
ATTN AWSR Lt. Col. Cornelius H. McGuiness

SAMSO/IN
Post Office Box 92960
Worldway Postal Center
Los Angeles, CA 90009
ATTN IND I. J. Judy

SAMSO/MN
Norton AFB, CA 92409
ATTN MNNG Capt. David J. Strobel
ATTN MNNG
ATTN MNNH

SAMSO/RS
Post Office Box 92960
Worldway Postal Center
Los Angeles, CA 90009
ATTN RSSE LTC Kenneth L. Gilbert

SAMSO/SK
Post Office Box 92960
Worldway Postal Center
Los Angeles, CA 90009
ATTN SKF Peter H. Stadler

Commander-in-Chief
Strategic Air Command
Offutt AFB, NB 68113
ATTN XPFS Maj. Brian G. Stephan
ATTN NRI-STINFO Library

University of California
Lawrence Livermore Laboratory
P.O. Box 808
Livermore, CA 94550
ATTN Tech Info Dept L-3
ATTN Lawrence Cleland L-156
ATTN Hans Kruger L-96
ATTN Joseph E. Keller, Jr. L-125

Los Alamos Scientific Laboratory
P.O. Box 1663
Los Alamos, NM 87545
ATTN Doc. Cont. for J. Arthur Freed

Sandia Laboratories
P.O. Box 5800
Albuquerque, NM 87115
ATTN DOC CON for 3141 Sandia Rpt Coll
ATTN DOC CON for Org 2110 J. A. Hood
ATTN DOC CON for Org 1933 F. N. Coppage

Department of Commerce
National Bureau of Standards
Washington, D.C. 20234
ATTN Judson C. French, A357 Tech
ATTN W. M. Bullis, A355 Tech
ATTN K. F. Galloway, A327 Tech

Aerojet Electro-Systems Co Div
Aerojet-General Corp
P.O. Box 296
Azusa, CA 91702
ATTN Thomas D. Hanscome

Aeronutronic Ford Corporation
Aerospace & Communications Ops
Aeronutronic Div
Fort & Jamboree Roads
Newport Beach, CA 92663
ATTN Tech Info Section
ATTN Ken C. Attinger

Aeronutronic Ford Corporation
Western Development Laboratories Div
3939 Fabian Way
Palo Alto, CA 94303
ATTN Samuel R. Crawford MS 531

Aerospace Corp
P.O. Box 92957
Los Angeles, CA 90009
ATTN Irving M. Garfunkel
ATTN J. Benveniste
ATTN Julian Reinheimer
ATTN S. P. Bower
ATTN W. Willis

AVCO Research & Systems Group
201 Lowell Street
Wilmington, MA 01887
ATTN Research Lib A830, Rm 7201

The BDM Corp
1920 Aline Ave
Vienna, VA 21180
ATTN T. H. Neighbors

The Bendix Corp
Communication Division
East Joppa Road - Towson
Baltimore, MD 21204
ATTN Document Control

The Bendix Corp
Research Laboratories Div
Bendix Center
Southfield, MI 48076
ATTN Max Frank
ATTN Mgr Prgm Dev Donald J. Niehaus

The Bendix Corp
Navigation and Control Div
Teterboro, NJ 07608
ATTN George Gartner

The Boeing Company
P.O. Box 3707
Seattle, WA 98124
ATTN David L. Dye MS 87-75
ATTN Aerospace Library
ATTN Howard W. Wicklein MS 17-11
ATTN Robert S. Caldwell 2R-00
ATTN Carl Rosenberg 2R-00
ATTN Itsu Arimura 2R-00

Booz-Allen and Hamilton, Inc.
106 Apple Street
New Shrewsbury, NJ 07724
ATTN Raymond J. Chrisner

California Inst. of Tech.
Jet Propulsion Lab
4800 Oak Park Grove
Pasadena, CA 91103
ATTN J. Bryden
ATTN A. G. Stanley

Charles Start Draper Laboratory, Inc.
68 Albany Street
Cambridge, MA 02139
ATTN Kenneth Fertig

Computer Sciences Corp
201 La Veta Drive, N.E.
Albuquerque, NM 87108
ATTN Richard H. Dickhaut

Cutler-Hammer, Inc.
AIL Div
Comac Road
Deer Park, NJ 11729
ATTN Central Tech Files Anne Anthony

The Dikewood Corp
1009 Bradbury Drive, S.E.
University Research Park
Albuquerque, NM 87106
ATTN L. Wayne Davis

E-Systems, Inc.
Greenville Div
P.O. Box 1056
Greenville, TX 75401
ATTN Library 8-50100

Effects Technology, Inc.
5383 Hollister Avenue
Santa Barbara, CA 93111
ATTN Edward John Steele

Fairchild Camera and Instrument Corp
464 Ellis Street
Mountain View, CA 94040
ATTN Sec Dept for 2-233 David K. Myers

Fairchild Industries, Inc.
Sherman Fairchild Technology Ctr
20301 Century Boulevard
Germantown, MD 20767
ATTN Mgr Config Data & Standards

Garrett Corp
P.O. Box 92248
Los Angeles, CA 90009
ATTN Robert E. Weir Dept 93-9

General Dynamics Corp
Electronics Div Orlando Operations
P.O. Box 2566
Orlando, FL 32802
ATTN D. W. Coleman

General Electric Company
Space Division
Valley Forge Space Center
Goddard Blvd King of Prussia
P.O. Box 8555
Philadelphia, PA 19101
ATTN Larry I. Chasen
ATTN John L. Andrews
ATTN Joseph C. Peden VFSC, Rm 4230M

General Electric Company
Re-entry & Environmental Systems Div
P.O. Box 7722
3198 Chestnut Street
Philadelphia, PA 19101
ATTN John W. Palchefsky Jr.
ATTN Robert V. Benedict

General Electric Company
Ordnance Systems
100 Plastics Avenue
Pittsfield, MA 01201
ATTN Joseph J. Reidl

General Electric Company
Tempo-Center for Advanced Studies
816 State Street (P.O. Drwr QQ)
Santa Barbara, CA 93102
ATTN M. Espig
ATTN DASIAC
ATTN Royden R. Rutherford

General Electric Company
P.O. Box 1122
Syracuse, NY 13201
ATTN CSP 0-7 L. H. Dee

General Electric Company
Aircraft Engine Group
Evendale Plant
Cincinnati, OH 45215
ATTN John A. Ellerhorst E 2

General Electric Company
Aerospace Electronics Systems
French Road
Utica. NY 13503
ATTN W. J. Patterson Drop 233
ATTN Charles M. Hewison Drop 624

General Electric Company - Tempo
ATTN: DASIAC
C/O Defense Nuclear Agency
Washington, D.C. 20305
ATTN William Alfonte

Georgia Institute of Technology
Georgia Tech Research Inst
Atlanta, GA 30332
ATTN R. Curry

Grumman Aerospace Corp
South Oyster Bay Road
Bethpage, NY 11714
ATTN Jerry Rogers Dept 533

GTE Sylvania, Inc.
Electronics Systems Grp - Eastern Div
77 A Street
Needham, MA 02194
ATTN James A. Waldon
ATTN Charles A. Thornhill Librarian
ATTN Leonard L. Blaisdell

GTE Sylvania, Inc.
189 B Street
Needham Heights, MA 02194
ATTN H & V Group Mario A. Nurefora
ATTN Herbert A. Ullman

Gulton Industries, Inc.
Engineered Magnetics Division
13041 Cerise Avenue
Hawthorne, CA 90250
ATTN Engnmagnetics Div

Harris Corp
Harris Semiconductor Div
P.O. Box 883
Melbourne, FL 32901
ATTN Wayne E. Abare MS 16-111
ATTN Carl F. Davis MS 17-220
ATTN T. L. Clark MS 4040

Hazeltine Corp
Pulaski Road
Green Lawn, NY 11740
ATTN Tech Info Ctr M. Waite

Honeywell Inc.
Government and Aeronautical
Products Division
2600 Ridgeway Parkway
Minneapolis, MN 55413
ATTN Ronald R. Johnson A1622

Honeywell Inc.
Aerospace Division
13350 U.S. Highway 19
St. Petersburg, FL 33733
ATTN M.S. 725-J Stacey H. Graff
ATTN Harrison H. Noble M.S. 725-5A

Honeywell Inc.
Radiation Center
2 Forbes Road
Lexington, MA 02173
ATTN Technical Library

Hughes Aircraft Company
Centinela and Teale
Culver City, CA 90230
ATTN John B. Singletary MS 6-D133
ATTN Billy W. Campbell MS 6-E-110
ATTN Kenneth R. Walker MS D157

Hughes Aircraft Company
Space Systems Div
P.O. Box 92919
Los Angeles, CA 90009
ATTN Edward C. Smith MS A620
ATTN William W. Scott MS A1080

IBM Corp
Route 17C
Owego, NY 13827
ATTN Frank Frankovsky

IIT Research Institute
10 West 35th Street
Chicago, IL 60616
ATTN Irving N. Mindel

Intl Tel & Telegraph Corp.
500 Washington Avenue
Nutley, NJ 07110
ATTN Alexander T. Richardson

IRT Corp
P.O. Box 81087
San Diego, CA 92138
ATTN R. L. Mertz
ATTN Ralph H. Stahl
ATTN Leo D. Cotter
ATTN MDC
ATTN John W. Harrity
ATTN J. L. Azarewicz

JAYCOR
205 S. Whiting Street, Suite 500
Alexandria, VA 22304
ATTN Robert Sullivan
ATTN Catherine Turesko

Johns Hopkins University
Applied Physics Laboratory
Johns Hopkins Road
Laurel, MD 20810
ATTN Peter E. Partridge

Kaman Sciences Corp
P.O. Box 7463
Colorado Springs, CO 80933
ATTN Albert P. Bridges
ATTN Donald H. Bryce
ATTN Jerry I. Lubell

Litton Systems, Inc.
Guidance & Control Systems Div
5500 Canoga Avenue
Woodland Hills, CA 91364
ATTN Val J. Ashby MS 67
ATTN John P. Retzler

Lockheed Missiles & Space Co., Inc.
P.O. Box 504
Sunnyvale, CA 94088
ATTN Benjamin T. Kimura Dept 81-14
ATTN Edwin A. Smith Dept. 85-85
ATTN Dept 81-01 G. H. Morris
ATTN L. Rossi Dept 81-64
ATTN Dept 85-85 Samual I. Taimuty

Lockheed Missiles and Space Company
3251 Hanover Street
Palo Alto, CA 94304
ATTN Tech Info Ctr D/Coll
ATTN John Crowley

LTV Aerospace Corp
Vought Systems Division
P.O. Box 6267
Dallas, TX 75222
ATTN Technical Data Center

LTV Aerospace Corp
Michigan Division
P.O. Box 909
Warren, MI 48090
ATTN Tech Lib

M.I.T. Lincoln Laboratory
P.O. Box 73
Lexington, MA 02173
ATTN Leona Loughlin Librarian A-082

Martin Marietta Aerospace
Orlando Division
P.O. Box 5837
Orlando, FL 32805
ATTN Mona C. Griffith Lib MP-30
ATTN Jack M. Ashford MP-537
ATTN William W. Mras MP-413
ATTN Richard Gaynor

McDonnell Douglas Corp
P.O. Box 516
St. Louis, MO 63166
ATTN Tech Lib
ATTN Tom Ender

Mission Research Corp
735 State Street
Santa Barbara, CA 93101
ATTN William C. Hart

Mission Research Corp-La Jolla
1150 Silverado Street
P.O. Box 1209
La Jolla, CA 92038
ATTN V. A. J. Van Lint
ATTN James Raymond

National Academy of Sciences
ATTN: National Materials Advisory Board
2101 Constitution Avenue
Washington, D.C. 20418
ATTN R. S. Shane Nat Materials Advsy

Northrop Corp
Electronic Div
1 Research Park
Palos Verdes Peninsula, CA 90273
ATTN Vincent R. Demartino
ATTN Boyce T. Ahlport

Northrop Corp
Northrop Research and Technology Ctr
3401 West Broadway
Hawthrone, CA 90250
ATTN Orlie L. Curtis, Jr.
ATTN J. R. Srour
ATTN David N. Pocock

Palisades Inst. for Rsch Services, Inc.
201 Varick Street
New York, NY 10014
ATTN Records Supervisor

Power Physics Corp
542 Industrial Way West
P.O. Box 626
Eatontown, NJ 07724
ATTN Mitchell Baker

R & D Associates
P.O. Box 9695
Marina Del Rey, CA 90291
ATTN S. Clay Rogers

Raytheon Company
Hartwell Road
Bedford, MA 01730
ATTN Gajanan H. Joshi Radar Sys Lab

Raytheon Company
528 Boston Post Road
Sudbury, MA 01776
ATTN Harold L. Flescher

RCA Corporation
Government & Commercial Systems
ASTRO Electronics Div
P.O. Box 800, Locust Corner
Princeton, NJ 08540
ATTN George J. Brucker

RCA Corporation
David Sarnoff Research Ctr
W. Windsor Twp
201 Washington Road, P.O. Box 432
Princeton, NJ 08540
ATTN K. H. Zaininger

RCA Corporation
Camden Complex
Front & Cooper Sts
Camden, NJ 08012
ATTN E. Van Keuren 13-5-2

Research Triangle Inst
P.O. Box 12194
Research Triangle Park, NC 27709
ATTN Eng Div Mayrant Simons Jr.

Rockwell International Corp
3370 Miraloma Ave
Anaheim, CA 92803
ATTN N. J. Rudie FA53
ATTN James E. Bell HA10
ATTN George C. Messenger FB61
ATTN K. F. Hull
ATTN L. Apodaca FA53

Rockwell International Corporation
5701 West Imperial Highway
Los Angeles, CA 90009
ATTN T. B. Yates

Rockwell International Corporation
Electronics Operations
Collins Radio Group
5225 C Avenue NE
Cedar Rapids, IA 52406
ATTN Alan A. Langenfeld
ATTN Dennis Sutherland
ATTN Mildred A. Blair

Sanders Associates, Inc.
95 Canal Street
Nashua, NH 03060
ATTN Moe L. Aitel NCA 1-3236

Science Applications, Inc.
P.O. Box 2351
La Jolla, CA 92038
ATTN Larry Scott
ATTN J. Robert Beyster
ATTN Victor Orphan

Simulation Physics, Inc.
41 "B" Street
Burlington, MA 01803
ATTN Roger G. Little

The Singer Company (Data Systems)
150 Totowa Road
Wayne, NJ 07470
ATTN Tech Info Ctr

Sperry Flight Systems Div
Sperry Rand Corp
P.O. Box 21111
Phoenix, AZ 85036
ATTN D. Andrew Schow

Sperry Rand Corp
Univac Div
Defense Systems Div
P.O. Box 3525 Mail Station 1931
St. Paul, MN 55101
ATTN James A. Inda MS 41T25

Sperry Rand Corp
Sperry Div
Sperry Gyroscope Div
Sperry Systems Management Div
Marcus Avenue
Great Neck, NY 11020
ATTN Paul Marraffino
ATTN Charles L. Craig EV

Stanford Research Inst
333 Ravenswood Ave
Menlo Park, CA 94025
ATTN Philip J. Dolan

Sundstrand Corp
4751 Harrison Avenue
Rockford, IL 61101
ATTN Curtis B. White

Texas Instruments, Inc.
P.O. Box 5474
Dallas, TX 75222
ATTN Donald J. Manus MS 72

TRW Systems Group
One Space Park
Redondo Beach, CA 90278
ATTN H. H. Holloway R1-2036
ATTN O. E. Adams R1-1144 (2 copies)
ATTN R. K. Plebuch R1-2078 (2 copies)
ATTN Tech Info Center/S-1930
ATTN Robert M. Webb R1-2410

TRW Systems Group
San Bernardino Operations
P.O. Box 1310
San Bernardino, CA 92402
ATTN F. B. Fay 527/710
ATTN Earl W. Allen

TRW Systems Group
P.O. Box 368
Clearfield, UT 84015
ATTN Donald W. Pugsley

United Technologies Corp
Hamilton Standard Div
Bradley International Airport
Windsor Locks, CT 06069
ATTN Raymond G. Giguere

Westinghouse Electric Corp
Defense and Electronic Systems Ctr
P.O. Box 1693
Friendship International Airport
Baltimore, MD 21203
ATTN Henry P. Kalapaca MS 3525

NBS-114A (REV. 7-73)

U.S. DEPT. OF COMM. BIBLIOGRAPHIC DATA SHEET	1. PUBLICATION OR REPORT NO. NBSIR 77-1235	2. Gov't Accession No.	3. Recipient's Accession No.

4. TITLE AND SUBTITLE

Some Aspects of Using an SEM for Total Dose Testing

5. Publication Date September 1977

6. Performing Organization Code

7. AUTHOR(S) K. F. Galloway and P. Roitman

8. Performing Organ. Report No. NBSIR-77-1235

9. PERFORMING ORGANIZATION NAME AND ADDRESS

NATIONAL BUREAU OF STANDARDS
DEPARTMENT OF COMMERCE
WASHINGTON, D.C. 20234

10. Project/Task/Work Unit No.

11. Contract/Grant No. DNA IACRO 77-809

12. Sponsoring Organization Name and Complete Address (Street, City, State, ZIP)

Defense Nuclear Agency
Washington, D.C. 20305

13. Type of Report & Period Covered

14. Sponsoring Agency Code

15. SUPPLEMENTARY NOTES

16. ABSTRACT *(A 200-word or less factual summary of most significant information. If document includes a significant bibliography or literature survey, mention it here.)*

This report addresses a number of aspects involved in using a Scanning Electron Microscope (SEM) for radiation testing of semiconductor devices. Problems associated with using the low energy electron beam to simulate ^{60}Co exposure and a method for estimating the total absorbed dose in critical device oxides are discussed. The method is based on the experimentally determined expression for electron energy dissipation versus penetration depth in solid materials of Everhart and Hoff. An appendix giving the method of estimating the total absorbed dose in a form suitable for ASTM deliberations is included.

17. KEY WORDS *(six to twelve entries; alphabetical order; capitalize only the first letter of the first key word unless a proper name; separated by semicolons)*

Electron beam energy deposition; ionizing radiation effects; radiation dose; radiation testing; semiconductor devices; scanning electron microscope.

18. AVAILABILITY

[X] Unlimited

[ ] For Official Distribution. Do Not Release to NTIS

[X] Order From Sup. of Doc., U.S. Government Printing Office Washington, D.C. 20402, SD Cat. No. C13

[ ] Order From National Technical Information Service (NTIS) Springfield, Virginia 22151

19. SECURITY CLASS (THIS REPORT)	21. NO. OF PAGES
UNCLASSIFIED	40
20. SECURITY CLASS (THIS PAGE)	**22. Price**
UNCLASSIFIED	$4.50

USCOMM-DC 29042-P74